remote sensing

MDPI

Article

Hierarchical Analysis of *Miombo* Woodland Spatial Dynamics in Lualaba Province (Democratic Republic of the Congo), 1990–2024: Integrating Remote Sensing and Landscape Ecology Techniques

Yannick Useni Sikuzani [1], Médard Mpanda Mukenza [2], John Kikuni Tchowa [3], Delphin Kabamb Kanyimb [4], François Malaisse [5] and Jan Bogaert [5,*]

[1] Ecology, Ecological Restoration and Landscape Unit, Faculty of Agronomics Sciences, University of Lubumbashi, Lubumbashi P.O. Box 1825, Democratic Republic of the Congo; sikuzaniu@unilu.ac.cd
[2] Department of Renewable Natural Resources Management, Faculty of Agronomic Sciences, Katumba Mwanke University of Technology, Lubumbashi P.O. Box 74, Democratic Republic of the Congo; m.mpanda@eraift-rdc.org
[3] Department of Plant Science, Faculty of Agricultural Sciences, University of Kolwezi, Kolwezi P.O. Box 57, Democratic Republic of the Congo; kikunitchowajohnw@gmail.com
[4] Regional Postgraduate School for Integrated Planning and Management of Forests and Tropical Territories, Kinshasa P.O. Box 15373, Democratic Republic of the Congo; delphinkabamb@gmail.com
[5] Biodiversity, Ecosystem and Landscape Unit, Gembloux Agro-Bio Tech, University of Liège, 5030 Gembloux, Belgium; malaisse1234@gmail.com
* Correspondence: j.bogaert@uliege.be

Abstract: Lualaba Province, located in the southeastern Democratic Republic of the Congo (DRC), consists of five territories with varied dominant land uses: agriculture (Dilolo, Kapanga, and Musumba in the west) and mining (Mutshatsha and Lubudi in the east). The province also includes protected areas with significant governance challenges. The tropical dry forests that cover the unique *Miombo* woodland of Lualaba are threatened by deforestation, which poses risks to biodiversity and local livelihoods that depend on these forests for agriculture and forestry. To quantify the spatio-temporal dynamics of Lualaba's landscape, we utilized Landsat images from 1990 to 2024, supported by a Random Forest Classifier. Landscape metrics were calculated at multiple hierarchical levels: province, territory, and protected areas. A key contribution of this work is its identification of pronounced deforestation trends in the unique *Miombo* woodlands, where the overall woodland cover has declined dramatically from 62.9% to less than 25%. This is coupled with a marked increase in landscape fragmentation, isolation of remaining woodland patches, and a shift toward more heterogeneous land use patterns, as evidenced by the Shannon diversity index. Unlike previous research, our study distinguishes between the dynamics in agricultural territories—which are particularly vulnerable to deforestation—and those in mining areas, where *Miombo* forest cover remains more intact but is still under threat. This nuanced distinction between land use types offers critical insights into the differential impacts of economic activities on the landscape. Our study also uncovers significant deforestation within protected areas, underscoring the failure of current governance structures to safeguard these critical ecosystems. This comprehensive analysis offers a novel contribution to the literature by linking the spatial patterns of deforestation to both agricultural and mining pressures while simultaneously highlighting the governance challenges that exacerbate landscape transformation. Lualaba's *Miombo* woodlands are at a critical juncture, and without urgent, coordinated intervention from local and international stakeholders, the ecological and socio-economic foundations of the region will be irreversibly compromised. Urgent action is needed to implement land conservation policies, promote sustainable agricultural practices, strengthen *Miombo* woodland regulation enforcement, and actively support protected areas.

Keywords: deforestation; biodiversity conservation; anthropogenic pressures; remote sensing; landscape analysis; protected areas

Citation: Useni Sikuzani, Y.; Mpanda Mukenza, M.; Kikuni Tchowa, J.; Kabamb Kanyimb, D.; Malaisse, F.; Bogaert, J. Hierarchical Analysis of *Miombo* Woodland Spatial Dynamics in Lualaba Province (Democratic Republic of the Congo), 1990–2024: Integrating Remote Sensing and Landscape Ecology Techniques. *Remote Sens.* **2024**, *16*, 3903. https://doi.org/10.3390/rs16203903

Academic Editor: Brenden E. McNeil

Received: 30 August 2024
Revised: 26 September 2024
Accepted: 14 October 2024
Published: 21 October 2024

1. Introduction

Dry forests play a crucial role in maintaining ecosystems, particularly in tropical and subtropical regions. These ecosystems cover approximately 40% of tropical areas and are home to exceptional biodiversity, with species adapted to water scarcity [1,2]. They are also recognized for their ability to store carbon and regulate the climate despite harsh climatic conditions [3,4]. In addition, dry forests provide essential ecosystem services, including preventing soil erosion and providing non-timber forest products that support local communities in food security and traditional medical care [5–7].

Dry tropical forests cover approximately one-sixth of the Earth's surface and half of Africa [8]. These ecosystems are among the most threatened, primarily due to human activities [9]. Among these ecosystems, *Miombo* woodlands, which dominate southern Africa, are vital for both biodiversity and local livelihoods. These woodlands are primarily composed of tree species from the genera *Brachystegia*, *Julbernardia*, and *Isoberlinia*, which belong to the *Caesalpionioideae* subfamily. These trees play a key role in maintaining soil fertility, supporting wildlife habitats, and providing essential resources, such as firewood, construction materials, and non-timber forest products for local communities [10]. Their dominance in *Miombo* woodlands is crucial for the ecological balance of these regions, as they are well-adapted to the dry climate and poor soils, contributing significantly to carbon storage and ecosystem resilience [11,12]. They cover an area of 2 million km^2, encompassing parts of Angola, the Democratic Republic of the Congo (DRC), Malawi, Mozambique, Tanzania, Zambia, and Zimbabwe [13]. This ecoregion is recognized as an important center of endemism, hosting over 8500 plant species, with more than 4000 being endemic [14]. These ecosystems play a vital role in maintaining biodiversity and supporting the livelihoods of local populations [15].

In 2000, *Miombo* woodlands accounted for nearly 23% of the total forest area in the DRC while representing 95.2% of the total forest cover in the Katanga region that same year [16,17]. Between 2000 and 2010, the Katanga region, which includes the current Lualaba Province following its subdivision, experienced a loss of approximately 350,900 hectares of forest due to the expansion of mining and subsistence activities, such as agriculture, the collection of non-timber forest products, and charcoal production. These activities were driven by a demographic explosion and rapid urbanization. [18–20]. In the Katanga region, the Lualaba Province exemplifies the decline of the *Miombo* woodland [21]. For decades, Lualaba has been closely linked to mining, which has marked its history. The discovery of valuable mineral resources attracted a significant workforce, leading to the rapid expansion of mining settlements within the *Miombo* woodland [22]. After the political independence of the DRC in 1960, these settlements experienced rapid spatial expansion without adequate planning, severely affecting the surrounding forests [23]. Subsequently, the increasing demand for land for agriculture led to massive deforestation in surrounding rural areas, triggering a cycle of environmental disruption [20,24]. The energy crisis, particularly the energy deficit associated with the rapid expansion of settlements, also played a crucial role in this accelerated deforestation. Indeed, the widespread use of charcoal as an energy source in urban areas intensified pressure on already fragile forest resources [25]. This situation has endangered the biodiversity of the region, affecting not only forests but also protected areas.

Among these protected areas, Potapov et al.'s [16] findings revealed that the greatest forest cover loss was observed within hunting reserves close to Kolwezi, where forest cover loss within several protected areas was close to 5% between 2000 and 2010. Indeed, most protected areas are small and trapped within a landscape dominated by agricultural or mining zones [26]. Consequently, due to land saturation at the periphery, these protected areas are constantly degrading under pressure from local populations, whose interests are generally not considered in management systems [21]. Finally, the creation of the Lualaba Province in 2015 exacerbated these challenges as persistent population growth continues to exert immense anthropogenic pressure on the remaining forest resources [20].

Monitoring deforestation in the Lualaba Province is of critical importance for several stakeholders. It helps the government of the DRC and environmental organizations track deforestation patterns, understand their evolution over time, and anticipate future threats to the environment [27]. This is vital not only for biodiversity conservation and climate regulation but also for the local populations whose livelihoods depend on the sustainable use of forest resources. Additionally, such monitoring supports global efforts to combat climate change by preserving carbon sinks and protecting the rich ecosystems that Lualaba harbors. With precise data, policymakers can take appropriate measures for the conservation and sustainable environmental management of forest ecosystems [28]. In this context, remote sensing provides extensive coverage, making it ideal for tracking deforestation on a large scale within a province. It also offers frequent data for continuous monitoring, which has been demonstrated in various studies [29–32]. These technologies enable the timely detection of changes in land use, supporting effective conservation strategies and policy-making [33–35]. Concurrently, applying landscape ecology analysis tools complements this and allows for understanding the ecological processes underlying spatio-temporal changes in landscapes, thus aiding in locating at-risk areas [36–38]. Hierarchical analysis of landscape dynamics, combining remote sensing and landscape ecology, is essential from the provincial to the local scale. It enables a nuanced understanding of spatial heterogeneity, ecological processes, and anthropogenic impacts across scales. This approach supports precise, scale-appropriate interventions in landscape management, conservation planning, and sustainable development, ensuring more effective ecological and socio-economic outcomes.

The general objective is to quantify the multiscale spatio-temporal dynamics of forest ecosystems within the Lualaba Province. We hypothesize that a multiscale analysis (province, territory, and protected area) using Landsat imagery will reveal significant trends in the spatial dynamics of landscapes in Lualaba Province between 1990 and 2023, with greater variability emerging as the spatial scale of analysis decreases. This occurs because finer scales capture more localized processes and subtle variations in land use and vegetation cover. We expect to observe an increase in deforested and fragmented areas, as well as alteration of the spatial pattern and connectivity of the *Miombo* woodland over time, including, notably, at the protected area scale due to the close-range impact of human activities (mining, urbanization, and agriculture).

2. Materials and Methods

2.1. Study Area

The Lualaba Province (7°38′14.80′′–11°44′20.82′′S and 21°44′43.19–27°11′16.11′′E) in the southeastern part of the DRC, covering 121,309 km^2, constitutes 5.2% of the national territory (Figure 1). It exhibits a diverse climate, featuring a warm, temperate climate in the eastern sector (Mutshatsha and Lubudi territories) and a more humid, tropical climate in the western areas (Kapanga, Dilolo, and Sandoa) [22]. The province experiences distinct rainy and dry seasons, spanning approximately five months from April to May. Its annual rainfall is around 1600 mm for the northwest compared to nearly 1200 mm for the eastern part of the province. The average annual temperature hovers around 25 °C [22,24]. The primary vegetation in the Lualaba Province encompass dry dense forests, edaphic dense forests, *Miombo* woodland, savannas, and aquatic environments [17,22]. The region's soils are notably diverse [39], with a prevalence of Ferralsols, Acrisols, and Arenosols. Named after the Congo River, the Lualaba Province is characterized by plateaus, with various rivers like Lufupa, Kalule, Lulua, Luao, Lubilanshi, Luashi, Dikulwe, Musonoi, and Mumonwezi playing pivotal roles in local life and the economy. Recent data suggest a population of 4.3 million inhabitants (2021), with an average household size of 6.1 and life expectancy at 58.2 years. In Lualaba Province, the poverty rate stands at 83%, while the unemployment rate is 85%. Additionally, the annual population growth rate is close to 4% [40]. The province's mining sector, including both industrial and artisanal mining, has flourished, fostering formal and informal activities like general trade, subsistence agriculture, and informal commerce [41]. As for the employment sector breakdown, agriculture accounts for a substantial 71.4%. Regarding access to modern healthcare services, only 15.4% of the population has such access, and the electrification rate remains extremely low at just 1% [40]. The province is composed of 5 territories, within which are located protected areas (Table 1).

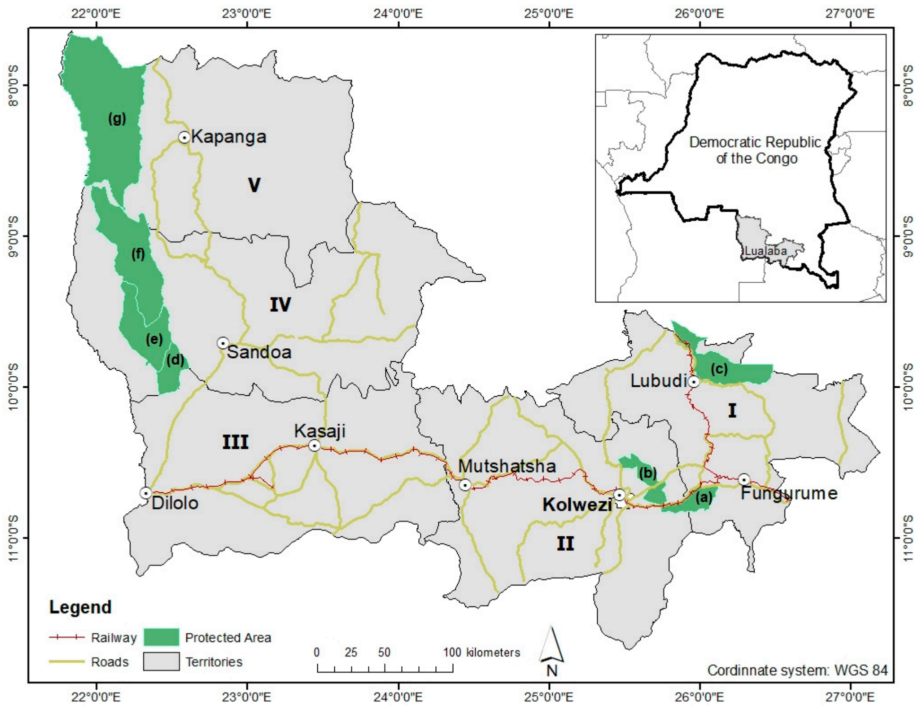

Figure 1. Geographical map of the Lualaba Province in the DRC, detailing its five territories, including key agricultural zones (IV) Sandoa, (V) Kapanga, and (III) Dilolo and major mining areas (I) Lubudi and (II) Mutshatsha. The map also identifies seven protected areas within Lualaba Province: (a) Basse Kando Hunting Domain (BKHD), (b) Lac Tshangalele Hunting Domain (LTHD), (c) Mulumbu Hunting Domain (MHD), (f) Alunda and Tutshokwe Hunting Reserve (ATHR), (d) Mwene Kay Hunting Domain (MKHD), (e) Mwene Musoma Hunting Domain (MMHD), and (g) Tshikamba Hunting Reserve (THR).

Table 1. Brief description of each territory in the province of Lualaba (DRC), its surface area, the economic activities of the population, and the protected area.

Territory	Area (km^2)	Population	Description
Lubudi	18,939	387,000	Economic activities include mining (artisanal and industrial), agriculture, and trade. The region is home to the rural municipality of Fungurume and the historic city of Bunkeya. Additionally, the territory encompasses the Hunting Domain of Mulumbu (993.56 km^2), and it is electrified with some paved roads.
Mutshatsha	18,859	1,268,500	Mining, agriculture, and commerce are key activities in this area, which includes the city of Kolwezi, the capital of the province. The territory is home to the Hunting Domain and Reserve of Basse Kando (479.18 km^2), as well as the Tshangalele Reserve (523.52 km^2). The territory is electrified and has some paved roads.
Sandoa	25,337	765,400	Agriculture and commerce thrive in this area. The territory, which lacks electricity and paved roads, is home to the Lunda-Tshokwe Hunting Domain (2345.27 km^2) and the Mwene-Kay Reserve (531.33 km^2).
Kapanga	25,509	1,255,600	Agriculture and commerce flourish in the territory, which is without electricity and paved roads. It is home to the Tshikamba Hunting Domain (4857.21 km^2).
Dilolo	25,648	623,500	Agriculture and commerce are prominent in this area, which includes the city of Kasaji. The territory, lacking electricity and paved roads, is home to the Mwene Musoma Hunting Domain (1303.99 km^2).

2.2. Data

Landsat images with a 30 m spatial resolution covering the period from 1990 to 2024 were used to map and quantify *Miombo* woodland cover loss in Lualaba Province. The analysis, divided into intervals (1990–1995, 1995–2001, 2001–2006, 2006–2010, 2010–2015, 2015–2020, and 2020–2024), highlights long-term trends and changes in landscape dynamics. The year 1990 marked the start of a political crisis, leading to looting and infrastructure destruction. The years 1995 and 2001 framed the Congo wars, causing significant population displacement to Lualaba. In 2006, The general elections in the DRC could have negatively impacted landscape dynamics by intensifying land disputes, accelerating deforestation, and disrupting conservation efforts due to political instability. The post-global economic crisis (2010) led to mine closures and uncertainty before the 2011 elections. In 2015, institutions were established in Kolwezi to govern the new Lualaba Province, and in 2020, there was a political regime change. The year 2024 provided a snapshot of the most recent landscape conditions. The selected Landsat images, captured during the dry season (June and July) to minimize cloud cover, were chosen for clear visibility and precise land cover interpretation. These images, representing surface reflectance data from Level 2 Collection 2 Tier 1 datasets, were selected based on availability, quality (cloud-free, no streaks), and the study's objectives [42]. Images from 1990, 1995, 2001, and 2006 were sourced from the Landsat 5 Thematic Mapper (TM) sensor, those from 2010 from the Landsat 7 Enhanced Thematic Mapper Plus (ETM+), and those from 2015 and 2024 from the Landsat 8 Operational Land Imager (OLI).

2.3. Classifications

The multi-temporal mosaic Landsat images were georeferenced to the UTM Zone 35S coordinate system using the WGS-84 reference ellipsoid appropriate for the study area and underwent extensive preprocessing. Radiometric calibration was initially applied to correct sensor biases and account for atmospheric effects, ensuring temporal consistency in readings [43,44]. Subsequently, geometric calibration addressed distortions caused by satellite movements, ensuring accurate pixel representation of the Earth's surface [45]. Atmospheric correction was then performed to eliminate effects, such as haze and scattering, thus enhancing surface reflectance analysis [46]. Additional radiometric preprocessing was conducted (for images from 2010 onward) to correct the spatial discontinuity that occurred in May 2003 following the Landsat 7 Scan Line Corrector (SLC) failure, which resulted in the loss of approximately 22% of data in each image scene. To mitigate this limitation, a "gap mask" technique was applied [47], effectively recovering missing data and ensuring the reliability and accuracy of subsequent analyses.

For improved analysis, a false-color composite was created by combining mid-infrared, near-infrared, and red bands, thus allowing for clearer differentiation of vegetation types [48]. Land cover was identified and codified for each scene, with Regions of Interest (ROIs) defined on the images based on field knowledge and GPS points collected during field surveys conducted in June and July 2024. For historical years (1990, 1995, 2001, 2006, 2010, 2015, and 2020), the ROIs were delineated using the imagery and local knowledge of the terrain. Each ROI was sized to the pixel size, allowing for representative sampling of different land cover types across the multi-temporal analysis. This approach ensures that the ROIs accurately reflect the diversity of land cover present in the study area, facilitating robust classification and analysis. For each land cover type, 200 ROIs were established on the images before they were classified, and 1000 GPS points per land cover type were collected for the field mission (the GPS receiver used to collect the points was accurate to within 3 m, model 64st).

These ROIs were strategically selected to avoid transitional areas, minimizing pixel mixing and enhancing result accuracy. These ROIs were then used to build a training model for the Random Forest classifier under Google Earth Engine (GEE) [49,50]. The Random Forest method, which relies on multiple decision trees, was implemented with a k-fold cross-validation approach to assess model robustness. Specifically, 70% of the data was used for training, while 30% was reserved for testing. A total of 150 trees were used in the final model. The accuracy of the model was evaluated using overall accuracy, producer's accuracy, and user's accuracy, achieving a final accuracy of more than 90%.

The land cover categories include "*Miombo* woodland": vegetation formation dominated by a sparse herbaceous layer under a forest stand 10 to 20 m high. This is land where tree cover predominates, with a minimum cover threshold of 0.05 to 1.0 hectare; "savanna", characterized by low tree density and predominance of herbaceous cover; "agriculture", covering harvested, abandoned, or areas occupied by annual and off-season crops; "built-up areas and bare soil", including bare lands and residential areas with minimal vegetation; and, finally, "other land cover types", such as water bodies and unclassified areas. The extensive archives of remote sensing data and GEE's powerful cloud computing resources ensured consistency and standardization of data collection procedures across different regions and datasets [49].

To evaluate the classification accuracy, after classifying multi-date Landsat images using Google Earth Engine (GEE), change maps were generated for the periods 1990–1995, 1995–2001, 2001–2006, 2006–2010, 2010–2015, 2015–2020, and 2020–2024. Following the validation recommendations of Olofsson et al. [51], reference points (1000 samples per period, independent from those used for classification) were extracted from these change maps for validation purposes. To enhance the reliability of these reference points, a field campaign was conducted in June and July 2024 to validate the recent data. For the historical periods, we relied on Google Earth Pro archives from 1990, 1995, 2001, 2006, 2010, 2015, and 2020. The sample collection on the change maps (reference points) followed a stratified approach to ensure an unbiased representation of different land cover classes. The samples were divided into nine strata: five stable land cover strata (stable *Miombo* woodland, stable savanna, stable agriculture, stable bare soil, and stable built-up areas) and four change strata (*Miombo* woodland loss, savanna gain, agriculture gain, and gain of bare soil and built-up areas). Cochran's method was employed to determine a sample size of 1000 points per period (independent from those used for classification) [52]. The distribution of points was proportional to the area of each stratum: 250 points for strata covering more than 40% of the area, 150 points for those covering between 10% and 40%, and 100 points for those representing less than 10%. Classification model validation was performed using rigorous statistical tests. An error matrix was generated in QGIS for each period, enabling the calculation of overall accuracies (OAs), user accuracies (UAs), and producer accuracies (PAs) for each class. The F1 score, which combines UA and PA [53], was preferred over the Kappa coefficient due to its superior sensitivity to class imbalances [54,55]. Error-corrected area estimates were calculated for each class, along with fixed 95% confidence intervals, guaranteeing the reliability of the results [51]. Version 3.26.1 of the QGIS software (developed by the worldwide QGIS community, Buenos Aires, Argentina) was used for all statistics.

2.4. Quantifying Spatio-Temporal Pattern Changes in Miombo Woodland Ecosystems

A range of landscape metrics were computed using Fragstats software version 4.2 (Developed by McGarigal, Amherst, MA, USA) to assess the influence of human activities on landscape structure and spatial patterns across three distinct scales: province, territory, and designated protected areas. The calculation of the class area, representing the proportional extent of specific land cover types within the landscape, served to identify the landscape matrix [56,57]. Edge density, indicating the total length of edge segments per hectare, was used to gauge landscape complexity. Higher edge density points to a more complex land cover type with distinct boundaries, while lower edge density suggests smoother boundaries [58]. The number of patches played a crucial role in assessing landscape fragmentation, where a higher count indicated fragmentation and dispersed distribution [59]. Further insights into spatial dispersion were gained through the average Euclidean distance to the nearest neighbor, measuring the average distance between patches and their closest neighbors. Additionally, the largest patch index, reflecting the size of the largest patch within a land cover type, was considered. A higher index value indicates that a particular land cover type forms larger, more connected patches beneficial for species needing extensive habitats or connectivity between patches for movement, migration, and genetic exchange [60]. The deforestation rate, derived from changes in the forest class area, provided insights into the intensity of human impacts on forest ecosystems [61]. The Shannon index, commonly used to assess the spatial arrangement of patches, was also computed. A Shannon value close to 0 indicates a highly uniform distribution of patches, while a value closer to 1 indicates a more dispersed distribution [58].

A decision tree approach was employed to identify the ecological processes driving observed spatio-temporal dynamics [62]. From a diachronic analysis, reductions in patch number and class area signify attrition, while an increase in class area alongside a decrease in patch number indicates aggregation. Unchanged patch numbers with increased class area suggest enlargement, whereas simultaneous growth in both metrics indicates the creation of new patches. Dissection is characterized by decreased class area and increased patch numbers, often due to linear disruptions with minimal area loss. Conversely, fragmentation involves an increase in patch numbers accompanied by significant class area loss. Perforation occurs when reductions in the class area lead to an increased total perimeter, while patch shrinkage occurs when the total perimeter remains constant. A consistent total perimeter with an unchanging patch number and class area signals a shift, while changes in the total perimeter suggest deformation. To distinguish between fragmentation and dissection, the ratio of the class area at different time points was analyzed. A ratio exceeding 0.75 indicated the dominance of dissection, whereas a ratio equal to or below 0.75 indicated prevalent fragmentation [63].

3. Results

3.1. Classification Accuracy and Mapping

The supervised classification of Landsat images using the Random Forest (RF) classifier achieved an Overall Accuracy (OA) exceeding 90% for each analyzed period, demonstrating its reliability in distinguishing between different land cover categories (Table 2). Both the user's accuracy (UA) and the producer's accuracy (PA) ranged between 90% and 100%, indicating the high quality of the classifications with minimal errors in class identification. Moreover, the application of a 95% confidence interval for estimating the stratified area of each land cover class across the different periods yielded a margin of error below 5%. This low level of uncertainty strengthens the credibility of the area estimates, suggesting that the results are both reliable and precise. The consistently high F1 scores for both UA and PA further validate the excellent performance of the RF classifier.

Table 2. Accuracy assessment and area estimate for the land cover and land cover change map based on the Landsat image supervised classification using the Random Forest classifier. MW: *Miombo* woodland stable; SV: savanna stable; AG: agriculture stable; BBS: built-up and bare soil stable; OT: other land cover stable; UA: user's accuracy; PA: producer's accuracy; CI: confidence interval. The change in the "OT" category was not assessed due to its relative stability throughout all periods. The F1 score was calculated as the harmonic mean of the UA and the PA.

1990–1995	**MW**	**SV**	**AG**	**BBS**	**OT**	**MW Loss**	**SV Gain**	**AG Gain**	**BBS Gain**
PA [%]	99.00	94.42	98.99	98.00	100	96.04	98.04	97.98	95.06
UA [%]	99.01	100	98.00	97.09	98.97	99.00	99.01	98.98	100
F1 [%]	99.00	97.13	98.49	97.54	99.48	97.50	98.52	98.48	97.47
Overall accuracy [%]	95.60								
Stratified estimators of area ± CI [% of total map area]									
Area [%]	17.20	19.17	8.76	9.12	9.29	8.20	8.90	9.67	9.69
95% CI	0.34	0.52	0.50	0.45	0.40	0.37	0.17	0.48	0.51

Table 2. *Cont.*

1990–1995	**MW**	**SV**	**AG**	**BBS**	**OT**	**MW Loss**	**SV Gain**	**AG Gain**	**BBS Gain**
1995–2001	MW	SV	AG	BBS	OT	MW Loss	SV Gain	AG Gain	OT Gain
PA [%]	93.58	100	98.05	100	100	100	95.88	100	100
UA [%]	97.14	100	99.01	99.03	96.08	96.3	89.42	99.03	96.08
F1 [%]	95.33	100.00	98.53	99.51	98.00	98.12	92.54	99.51	98.00
Overall accuracy [%]	98.40								
Stratified estimators of area ± CI [% of total map area]									
Area [%]	18.30	18.98	8.30	9.27	8.60	8.20	10.21	8.95	9.21
95% CI	0.35	0.47	0.33	0.45	0.28	0.35	0.33	0.33	0.41
2001–2006	MW	SV	AG	BBS	OT	MW Loss	SV Gain	AG Gain	OT Gain
PA [%]	97.02	100	96.04	98.04	97.98	95.06	100	98.9796	93.578
UA [%]	99.02	98.97	99	99.01	98.98	100	99.0196	96.0396	97.1429
F1 [%]	98.01	99.48	97.50	98.52	98.48	97.47	99.51	97.49	95.33
Overall accuracy [%]	96.61								
Stratified estimators of area ± CI [% of total map area]									
Area [%]	17.10	19.20	8.51	9.20	8.62	9.00	8.60	8.10	9.91
95% CI	0.48	0.42	0.47	0.36	0.33	0.10	0.35	0.23	0.33
2006–2010	MW	SV	AG	BBS	OT	MW Loss	SV Gain	AG Gain	OT Gain
PA [%]	98.06	99.03	100	98.04	100	100	99.03	97.8	97.35
UA [%]	98.54	100	99	100	98.02	100	100	100	99.1
F1 [%]	98.30	99.51	99.50	99.01	99.00	100.00	99.51	98.89	98.22
Overall accuracy [%]	98.30								
Stratified estimators of area ± CI [% of total map area]									
Area [%]	18.00	19.02	8.80	8.95	9.07	9.40	8.37	9.79	8.60
95% CI	0.45	0.50	0.40	0.36	0.35	0.35	0.35	0.37	0.40
2010–2015	MW	SV	AG	BBS	OT	MW Loss	SV Gain	AG Gain	OT Gain
PA [%]	98	96	98.11	98.1	100	100	98.04	97.98	97.06
UA [%]	97.09	98.06	99.05	99.04	98.99	95.1	99.01	98.98	100
F1 [%]	97.54	97.02	98.58	98.57	99.49	97.49	98.52	98.48	98.51
Overall accuracy [%]	98.91								
Stratified estimators of area ± CI [% of total map area]									
Area [%]	18.00	19.36	9.23	9.00	8.43	9.81	8.72	8.25	9.19
95% CI	0.60	0.51	0.40	0.44	0.26	0.31	0.30	0.40	0.50
2015–2020	MW	SV	AG	BBS	OT	MW Loss	SV Gain	AG Gain	OT Gain
PA [%]	99.09	100	98.97	93.58	100	98.05	100	98.06	93.58
UA [%]	100	99.02	96.04	97.14	100	99.01	97.06	98.06	97.14
F1 [%]	99.54	99.51	97.48	95.33	100.00	98.53	98.51	98.06	95.33
Overall accuracy [%]	97.51								
Stratified estimators of area ± CI [% of total map area]									
Area [%]	18.38	17.90	9.30	9.21	8.66	9.21	9.15	9.00	9.21
95% CI	0.45	0.44	0.50	0.65	0.38	0.28	0.33	0.36	0.21
2020–2024	MW	SV	AG	BBS	OT	MW Loss	SV Gain	AG Gain	OT Gain
PA [%]	100	98.04	100	100	100	100	100	100	98.08
UA [%]	100	100	98.02	100	98.02	100	100	99.06	98.08
F1 [%]	100.00	99.01	99.00	100.00	99.00	100.00	100.00	99.53	98.08
Overall accuracy [%]	98.45								

Table 2. *Cont.*

1990–1995	MW	SV	AG	BBS	OT	MW Loss	SV Gain	AG Gain	BBS Gain
Stratified estimators of area ± CI [% of total map area]									
Area [%]	17.30	18.98	9.51	9.00	8.87	9.00	9.42	8.94	9.00
95% CI	0.35	0.37	0.40	0.45	0.28	0.30	0.35	0.37	0.39

The visual analysis of land cover maps (Figure 2) reveals a gradual regression of forested areas in the Lualaba province between 1990 and 2024. This forest (*Miombo* woodland) decline is particularly pronounced along a west–east gradient, where previously forested areas are progressively being replaced by anthropogenic land cover classes, especially savannas, whose expansion is both rapid and striking. This phenomenon highlights the increasing pressures exerted by human activities on natural ecosystems. Nevertheless, despite this widespread trend of deforestation, forest fragments persist in the southeastern part of the province, indicating the resilience of certain forested areas in the face of anthropogenic expansion.

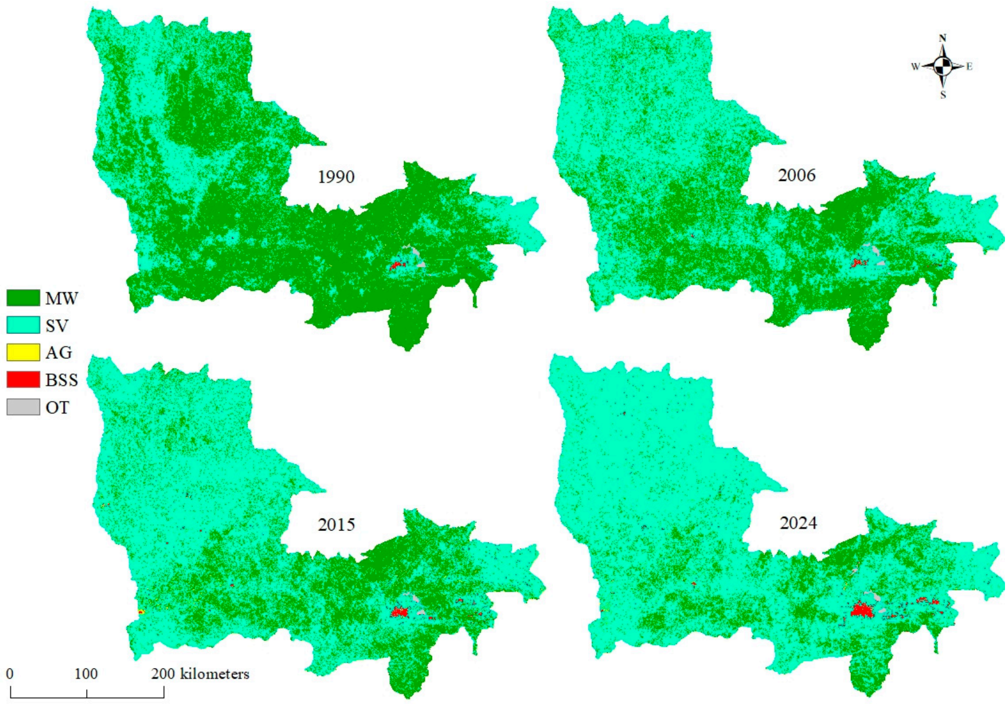

Figure 2. Spatial mapping of land cover dynamics in the Lualaba province landscape from 1990 to 2024, utilizing supervised classification of Landsat images with the Random Forest classifier. The land cover classes are denoted as follows: MW (*Miombo* woodland), SV (savanna), AG (agriculture), BBS (built-up and bare soil), and other land cover. Intermediate dates not displayed on this map did not exhibit significant perceptible changes in the landscape.

3.2. Landscape Composition Dynamics

3.2.1. Dynamics of Land Cover Composition in Lualaba Province and Its Territories

The multiscale landscape analysis from 1990 to 2024 reveals significant dynamics across the five territories of Lualaba province (Figure 3). Overall, *Miombo* woodland cover has notably decreased, dropping from 62.90% in 1990 to 24.59% in 2024, with an annual deforestation rate of −1.13% at the provincial level (A). Simultaneously, savannas have expanded considerably, increasing from 36.47% to 75.97%, while agricultural land and built-up areas have slightly risen to 1.78% and 1.09%, respectively. Similar trends are observed in Lubudi territory (B), where *Miombo* woodland cover has significantly decreased from 85.11% to 32.05% (i.e., an annual deforestation rate of −1.56%), accompanied by an expansion of savannas from 14.66% to 63.69%. Agricultural lands and built-up areas have also modestly increased. In Mutshatsha territory (C), deforestation is even more pronounced, with *Miombo* woodland cover declining from 84.52% to 32.81% (i.e., annual deforestation rate of −1.52%). During the same period, savannas expanded from 13.75% to 65.00%, and agricultural lands and built-up areas saw a slight increase. In Dilolo territory (D), *Miombo* woodland cover has decreased from 71.14% to 27.17% (i.e., annual deforestation rate of −1.29%), while savannas have continued their expansion, reaching 69.68% in 2024. Agricultural lands increased to 2.76%, while built-up areas remain limited. Additionally, in Sandoa territory (E), *Miombo* woodland cover has significantly declined from 52.56% to 12.80% (i.e., annual deforestation rate of −1.16%), with a concomitant increase in savannas from 47.11% to 85.19%. Agricultural lands and built-up areas have shown little change, reaching 1.38% and 0.56%, respectively. Finally, in Kapanga territory (F), *Miombo* woodland cover has drastically decreased from 49.66% to 5.57% (i.e., annual deforestation rate of −1.29%), while savannas have experienced substantial expansion, reaching 92.55% in 2024. In this territory, agricultural lands and built-up areas occupy less space in 2024. Across the five territories studied, the average annual deforestation rate between 1990 and 2024 is −1.36%.

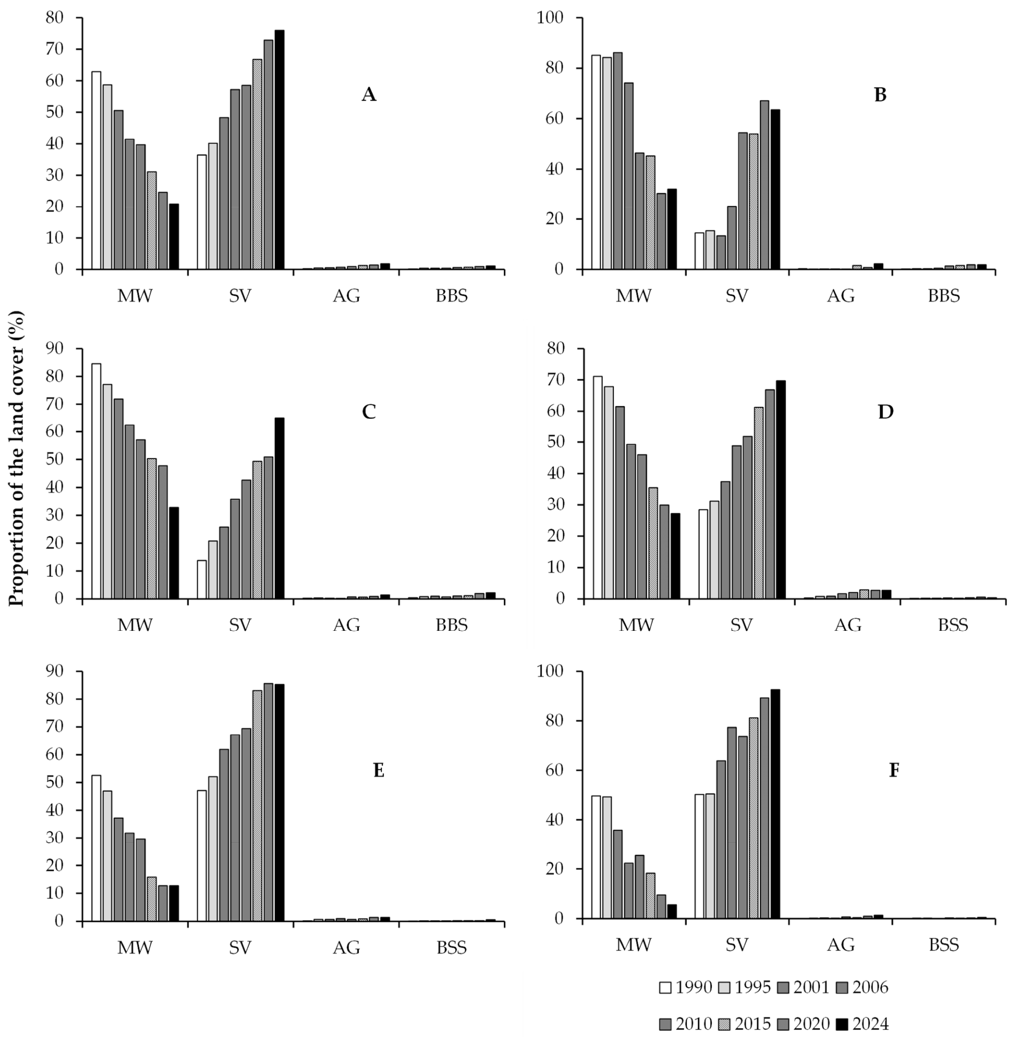

Figure 3. Landscape composition evolution in Lualaba province (**A**) (DRC) and their territories, (**B**) Lubudi, (**C**) Mutshatsha, (**D**) Dilolo, (**E**) Sandoa, and (**F**) Kapanga, from 1990 to 2024. MW (*Miombo* woodland), SV (savanna), AG (agriculture), and BBS (built-up and bare soil). The total landscape proportion in Lualaba province and for each territory does not sum to 100% as other land cover classes were excluded from the analyses due to their relatively stable nature.

Moreover, the global analysis of landscape diversity indices in Lualaba province indicates generally stable diversity with notable variations (Figure 4). From 1990 to 1995, diversity is homogeneous and high. However, from 2001 onwards, some territories exhibit a temporary increase, but diversity decreases in several areas from 2015, particularly in Kapanga. By 2024, diversity is low in Kapanga but stable in other territories, reflecting changes in landscape management and environmental conditions, such as deforestation rates or conservation efforts.

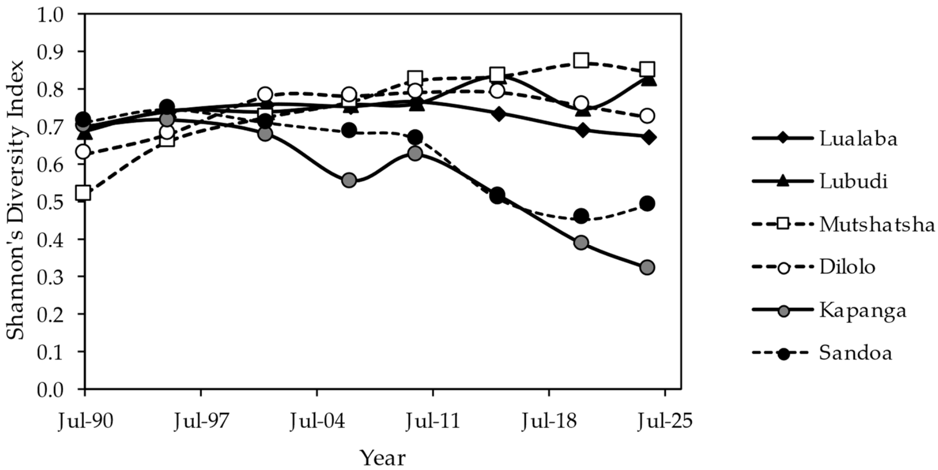

Figure 4. Dynamics of landscape diversity in Lualaba province (DRC) and its territories (Lubudi, Mutshatsha, Dilolo, Kapanga, and Sandoa). The overall landscape of Lualaba province has remained relatively stable between 1990 and 2024, though with notable variations during this period.

3.2.2. Dynamics of Land Cover Composition within Protected Areas in Lualaba Province

The analysis of land use data within the seven protected areas of Lualaba Province from 1990 to 2024 highlights concerning deforestation and significant conversion of *Miombo* woodland into savannas (Figure 5). The Basse Kando Hunting Domain (A) saw its *Miombo* woodland cover drop from 78.51% in 1990 to just 4.35% in 2024 (i.e., an annual deforestation rate of −2.18%). This loss was particularly pronounced after 2010, with a parallel increase in savannas from 20.87% to 78.27%. Simultaneously, built-up areas and bare soils expanded, reaching 15.11% in 2024. Similarly, the Lac Tshangalele Hunting Domain (B) experienced a significant reduction in *Miombo* woodlands, decreasing from 39.07% in 1990 to 2.18% in 2024 (i.e., an annual deforestation rate of −1.1). This decline accelerated after 2006, while savannas more than doubled, covering 57.11%. The growth of built-up areas reflects an intensification of human activities. Furthermore, the Mulumbu Hunting Domain (C) saw its *Miombo* woodland cover decrease by nearly 50%, from 62.78% in 1990 to 13.09% in 2024 (i.e., an annual deforestation rate of −1.46). This reduction was particularly marked between 2010 and 2020, with savannas expanding to cover 85.99%, becoming the dominant land cover. Similarly, the Alunda and Tutshokwe Hunting Reserve (D) recorded a significant decline in *Miombo* woodland cover, dropping from 51.64% in 1990 to 7.12% in 2024 (i.e., annual deforestation rate of −1.30). Savannas nearly doubled, representing 91.46% in 2024, illustrating a massive *Miombo* woodland conversion. The Mwene Kay Hunting Domain (E) also suffered a major loss in *Miombo* woodland cover, decreasing from 64.86% in 1990 to 15.89% in 2024 (i.e., an annual deforestation rate of −1.40). This reduction was accompanied by an increase in savannas, which covered 82.73% of the area in 2024. Similarly, the Mwene Musoma Hunting Domain (F) recorded a notable reduction in its *Miombo* woodlands, from 48.74% in 1990 to 9.26% in 2024 (i.e., an annual deforestation rate of −1.16). Savannas nearly doubled, reaching 90.28%, indicating a significant loss of *Miombo* woodland cover, declining from 38.44% in 1990 to 7.53% in 2024 (i.e., an annual deforestation rate of −0.90). Savannas increased to 90.59%, while built-up areas and bare soils experienced slight expansion. Across the seven protected areas studied, the average annual deforestation rate between 1990 and 2024 is −1.36%.

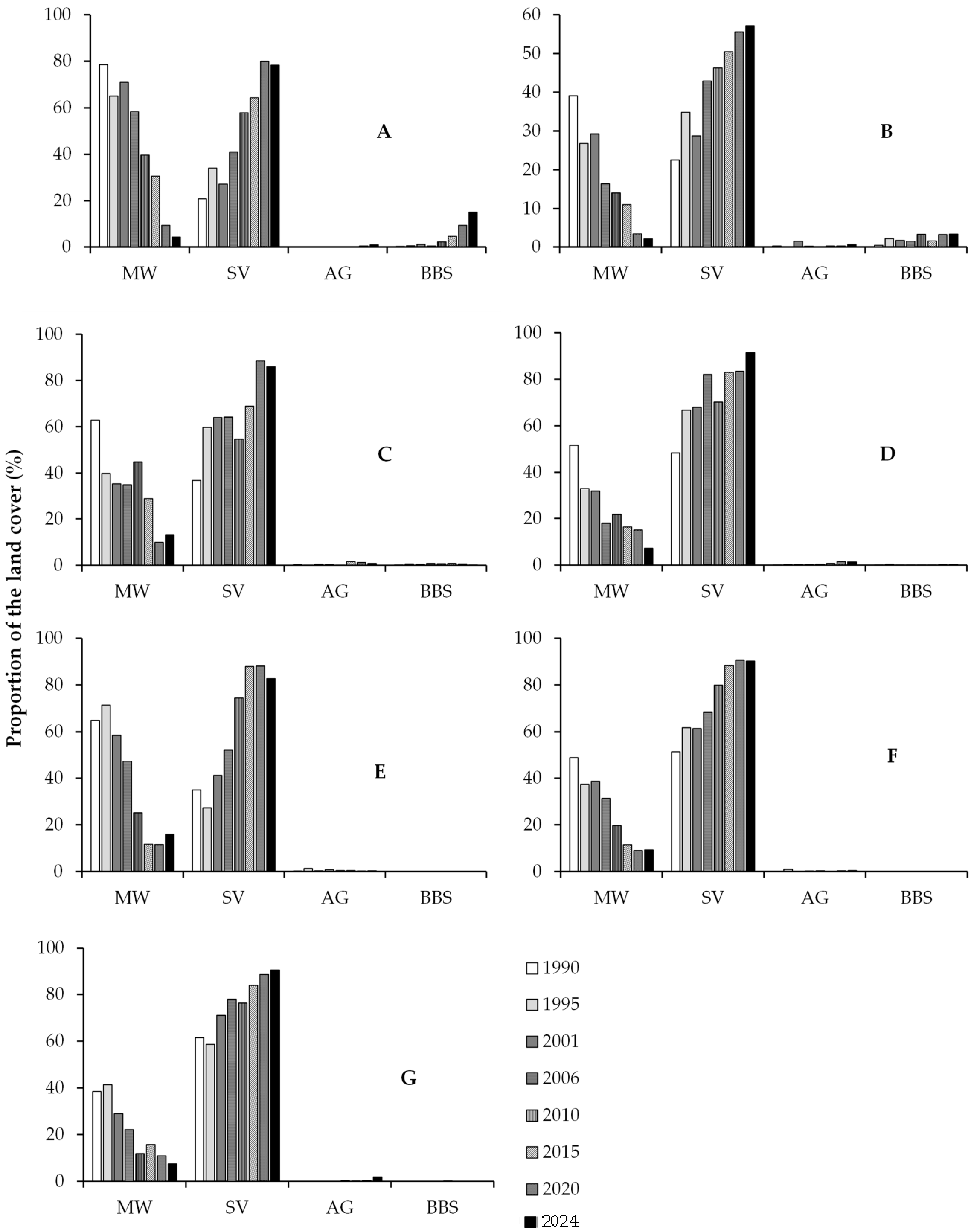

Figure 5. Landscape composition evolution in protected areas in Lualaba province from 1990 to 2024: The Basse Kando Hunting Domain (**A**); the Lac Tshangalele Hunting Domain (**B**); the Mulumbu Hunting Domain (**C**); the Alunda and Tutshokwe Hunting Reserve (**D**); The Mwene Kay Hunting Domain (**E**); the Mwene Musoma Hunting Domain (**F**); the Tshikamba Hunting Reserve (**G**). MW (*Miombo* woodland), SV (savanna), AG (agriculture) and BBS (built-up and bare soil). The total landscape proportion for each protected area does not sum to 100% as other land cover classes were excluded from the analyses due to their relatively stable nature.

The analysis of landscape diversity within Lualaba's protected areas reveals distinct trends (Figure 6). The Basse Kando Hunting Domain (BKHD) and the Mulumbu Hunting Domain (MHD) show an increase in landscape diversity. Conversely, the Alunda and Tutshokwe Hunting Reserve (ATHR), the Mwene Musoma Hunting Domain (MMHD), and the Mwene Kay Hunting Domain (MKHD) exhibit a significant reduction in diversity. The Lac Tshangalele Hunting Domain (LTHD) maintains high and stable diversity, while the Tshikamba Hunting Reserve (THR) shows declines and fluctuations, indicating potential management challenges for habitats. These results underscore the significant variations in landscape management and condition within the protected areas.

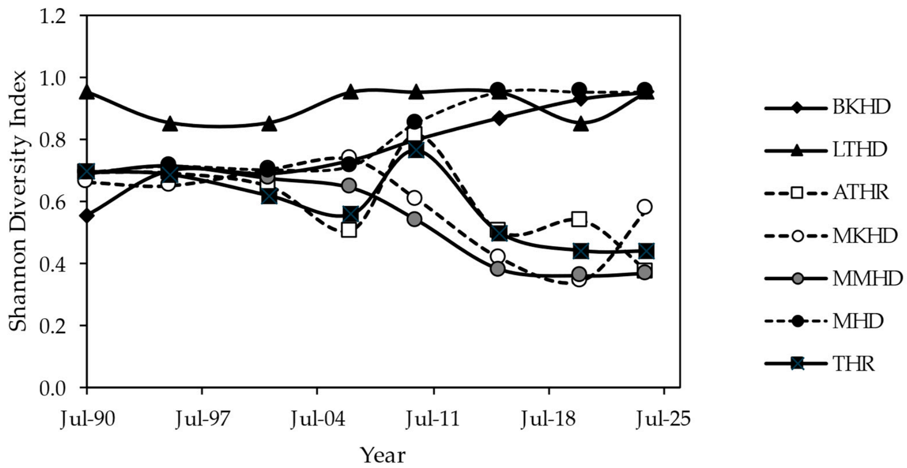

Figure 6. Dynamics of landscape diversity in the protected areas of Lualaba Province between 1990 and 2024. The protected areas have experienced variations in landscape homogeneity and heterogeneity over this period. Basse Kando Hunting Domain (BKHD), Lac Tshangalele Hunting Domain (LTHD), Mulumbu Hunting Domain (MHD), Alunda and Tutshokwe Hunting Reserve (ATHR), Mwene Kay Hunting Domain (MKHD), Mwene Musoma Hunting Domain (MMHD), and Tshikamba Hunting Reserve (THR).

3.3. Analysis of the Spatial Pattern Dynamics

Applying the decision tree model of Bogaert et al. [62] (Figure 7A,B), our analysis reveals that, except for Lubudi and Mutshatsha, the *Miombo* woodland in the Lualaba Province experienced an attrition process from 1990 to 1995, characterized by a decrease in class area (CA) followed by a reduction in the number of patches (PN). Lubudi and Mutshatsha, on the other hand, underwent dissection (ratio 0.95 > 0.75) due to a decline in CA coupled with an increase in PN. From 1995 to 2001, *Miombo* woodland attrition continued in Lualaba province, while dissection (ratio 0.87 > 0.75) was observed in Mutshatsha, Dilolo, and Sandoa. Concurrently, Kapanga faced fragmentation (ratio 0.72 < 0.75) due to reduced CA and increased PN, whereas Lubudi territory experienced aggregation, with a decrease in PN followed by an increase in CA. Between 2001 and 2006, dissection (ratio 0.84 > 0.75) prevailed across Lualaba province, except in Kapanga, where fragmentation (ratio 0.62 < 0.75) occurred because of increased PN and decreased CA. During 2006–2010, dissection (ratio 0.90 > 0.75) persisted in Lualaba, Mutshatsha, Dilolo, and Sandoa, while Lubudi was marked by fragmentation (ratio 0.62 < 0.75) and Kapanga by aggregation.

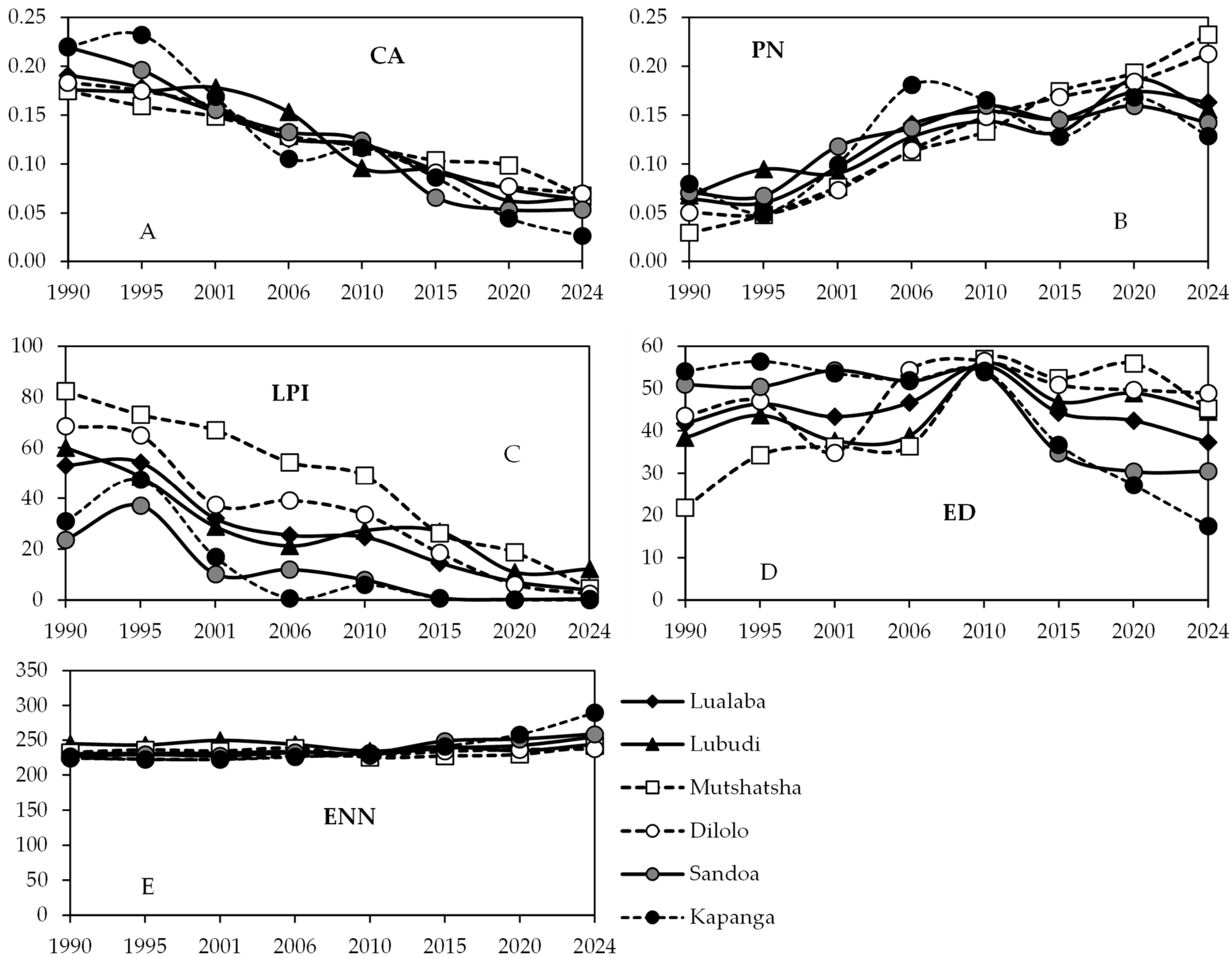

Figure 7. Dynamics of *Miombo* woodland spatial patterns (1990–2024). (**A**) displays the class area (CA, in km^2) of *Miombo* woodlands, with absolute values calculated by dividing the total *Miombo* woodland area for each year by the sum of *Miombo* woodland areas across all studied years. (**B**) illustrates the patch number (PN, also in absolute values) of *Miombo* woodland patches across the landscapes of Lualaba Province and its territories from 1990 to 2024. The variations in CA and PN during this period enabled the identification of spatial transformation processes, which were analyzed using the decision tree algorithm developed by Bogaert et al. [62]. (**C**) shows the evolution of the largest patch index (LPI, in %), which indicates the proportion of the landscape occupied by the largest *Miombo* woodland patch. (**D**) depicts the edge density (ED, in m/ha), reflecting the amount of edge habitat in relation to the *Miombo* woodland area. Finally, (**E**) presents the Mean Euclidean Nearest-Neighbor Distance (ENN, in meters), which measures the average distance between the nearest neighboring patches, providing insights into *Miombo* woodland connectivity.

From 2010 to 2015, attrition impacted *Miombo* woodland land cover in the entire province, as well as in Lubudi, Sandoa, and Kapanga, linked to decreases in both CA and PN. In Dilolo and Mutshatsha, dissection (ratio 0.82 > 0.75) was observed, driven by increased PN and decreased CA. Between 2015 and 2020, suppression was identified in Lualaba and Dilolo, while Lubudi and Kapanga experienced fragmentation (ratio 0.59 < 0.75), and Mutshatsha faced dissection due to decreased CA and increased PN. Finally, from 2020 to 2024, suppression affected Lualaba and Kapanga, Mutshatsha experienced fragmentation (ratio 0.68 < 0.75), and Dilolo underwent dissection (ratio 0.90 > 0.75), with Lubudi and Sandoa showing aggregation due to slight increases in CA followed by reductions in PN.

Between 1990 and 2024, the Lualaba Province and its territories witnessed a dramatic decline in *Miombo* woodland cover, with the largest patch of *Miombo* woodland plummeting from 53.1% in 1990 to just 3.98% in 2024 (Figure 7C), highlighting massive and concerning deforestation. Territories like Lubudi and Mutshatsha exhibited similar trends, with significant declines noted, especially after 2001. Dilolo, Sandoa, and Kapanga have nearly lost all of their *Miombo* woodlands, reaching a value of the largest patch near zero by 2024. In parallel, edge density (ED) in the province exhibited fluctuations (Figure 7, Panel D). Across all territories, ED decreased between 1990 and 2023, while reaching its highest value in 2010. Lubudi saw an initial increase in ED up to 2010 (55.95), followed by a slight decrease, reflecting initial fragmentation followed by stabilization. Mutshatsha's ED rose significantly from 21.80 in 1990 to 55.90 in 2020, then slightly declined, indicating substantial mid-period fragmentation. Dilolo followed a similar trend, with an increase until 2010 (56.50) and a slight decrease thereafter. Sandoa exhibited high and stable ED until 2010, then a marked decrease. Kapanga experienced a continuous decline in ED from 54.07 in 1990 to 17.42 in 2024.

Additionally, the average distance between *Miombo* woodland fragments increased from 230.53 m in 1990 to 254.47 m in 2024, reflecting growing *Miombo* woodland fragmentation at the provincial level (Figure 7E). Lubudi's distance remained relatively stable, from 244.72 m in 1990 to 244.17 m in 2024, indicating consistent fragmentation. In Mutshatsha, the average distance rose from 232.21 m in 1990 to 242.18 m in 2024, signaling increased fragmentation. Dilolo's distance slightly increased from 225.03 m in 1990 to 237.57 m in 2024, showing moderate fragmentation. Sandoa experienced a notable distance increase, from 226.57 m in 1990 to 258.56 m in 2024. In Kapanga, the average gap size increased significantly from 224.12 m in 1990 to 289.88 m in 2024, illustrating heightened fragmentation and larger distances between *Miombo* woodland fragments, likely driven by increased deforestation or land use changes.

Furthermore, our results reveal a complex evolution of spatial *Miombo* woodland transformation processes within protected areas in the Lualaba Province from 1990 to 2024 (Figure 8A,B). Between 1990 and 1995, *Miombo* woodlands in the MKHD and THR experienced an aggregation process, characterized by an increase in CA followed by a decrease in PN. Conversely, other protected areas showed an increase in PN and a decrease in CA, indicating a shift to dissection for ATHR and MMHD (ratio 0.79 > 0.75) and fragmentation (ratio 0.59 < 0.75) for BKHD, LTHD, and MHD. In the subsequent period, from 1995 to 2001, a notable change occurred in THR, where *Miombo* woodlands underwent fragmentation (ratio 0.69 < 0.75), driven by a decrease in CA combined with an increase in PN. Concurrently, *Miombo* woodlands in LTHD, MHD, and MKHD experienced dissection (ratio 0.79 > 0.75), while ATHR, BKHD, and MMHD observed the creation of *Miombo* woodland patches, marked by a simultaneous increase in CA and PN.

From 2001 to 2006, dissection dominated across all studied protected areas (ratio 0.83 > 0.75), except for BKHD and MHD, which experienced fragmentation (ratio 0.56 < 0.75). These transformations resulted from an increase in PN followed by a decrease in CA, a recurrent pattern continuing to shape *Miombo* woodland ecosystems. The period from 2006 to 2010 introduced the creation of the *Miombo* woodland's patches in LTHD and MHD due to a concurrent increase in CA and PN. Simultaneously, attrition was observed in ATHR and THR, marked by decreases in both CA and PN. However, MKHD and MMHD were characterized by fragmentation (ratio 0.58 < 0.75), while BKHD showed a dissection process (ratio 0.85 > 0.75), both characterized by an increase in PN. Between 2010 and 2015 in THR, *Miombo* woodland aggregation was observed, which resulted from a decrease in PN followed by an increase in CA, whereas other protected areas (ATHR, BKHD, LTHD, MHD, MKHD, and MMHD) experienced attrition of *Miombo* woodland patches resulting from an increase in PN and CA, enhancing the diversity of *Miombo* woodland dynamics. Between 2015 and 2020, fragmentation (ratio 0.30 < 0.75) was noted in ATHR, BKHD, THR, and LTHD due to increased PN and decreased CA. Meanwhile, MHD and MMHD experienced dissection of *Miombo* woodland patches (ratio 0.84 > 0.75), and MKHD underwent attrition resulting from an increase in PN followed by a decrease in CA, illustrating the complexity of spatial interactions in these zones. Finally, from 2020 to 2024, attrition of *Miombo* woodland patches dominated in ATHR, BKHD, and MHD, while THR faced fragmentation (ratio 0.30

< 0.75), which resulted from an increase in PN followed by a decrease in CA. MKHD and MMHD saw a spatial creation process, and LTHD experienced aggregation, concluding this analysis of *Miombo* woodland transformations with an illustration of varied and dynamic spatial trends in protected areas.

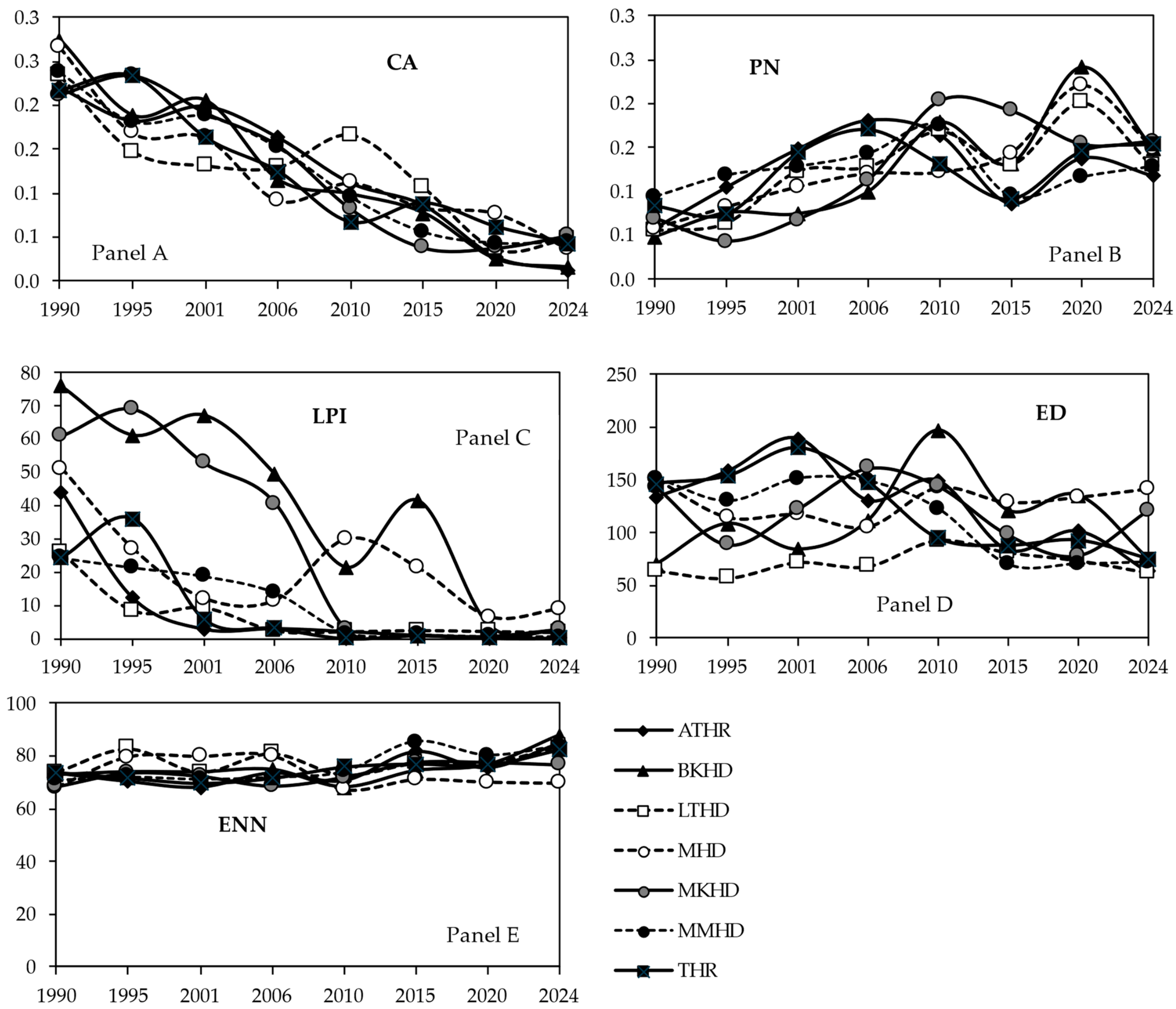

Figure 8. Dynamics of *Miombo* woodland spatial patterns in protected areas of Lualaba Province (1990–2024). (**A**) displays the class area (CA, in km^2) of *Miombo* woodlands, with absolute values calculated by dividing the total *Miombo* woodland area for each year by the sum of *Miombo* woodland areas across all studied years. (**B**) illustrates the patch number (PN, also in absolute values) of *Miombo* woodland patches across the protected areas in Lualaba Province from 1990 to 2024. The variations in CA and PN during this period enabled the identification of spatial transformation processes, which were analyzed using the decision tree algorithm developed by Bogaert et al. [62]. (**C**) shows the evolution of the largest patch index (LPI, in %), which indicates the proportion of the landscape occupied by the largest *Miombo* woodland patch. (**D**) depicts the edge density (ED, in m/ha), reflecting the amount of edge habitat in relation to *Miombo* woodland area. Finally, (**E**) presents the Mean Euclidean Nearest-Neighbor Distance (ENN, in meters), which measures the average distance between the nearest neighboring patches, providing insights into *Miombo* woodland connectivity. Basse Kando Hunting Domain (BKHD), Lac Tshangalele Hunting Domain (LTHD), Mulumbu Hunting Domain (MHD), Alunda and Tutshokwe Hunting Reserve (ATHR), Mwene Kay Hunting Domain (MKHD), Mwene Musoma Hunting Domain (MMHD), and Tshikamba Hunting Reserve (THR).

From 1990 to 2024, large *Miombo* woodland patches within protected areas drastically diminished, with the largest patches' index dropping to nearly zero in ATHR, BKHD, MMHD, and THR, with less pronounced declines in MKHD and LTHD (Figure 8C). MHD showed a slight recovery after 2010, but it remains at very low levels. Concurrently, the high edge density (ED) reflects increased *Miombo* woodland fragmentation over time. Despite initially high ED values, both ATHR and MMHD experienced a decrease in ED, whereas BKHD exhibited a significant rise until 2010, followed by a slight decline. LTHD, on the other hand, maintained a relatively stable ED with a slight upward trend (Figure 8D). MHD and MKHD showed fluctuations but generally followed an increasing trend in ED, while THR displayed a continuous rise, indicating ongoing fragmentation. This pattern is further supported by the Mean Euclidean Nearest-Neighbor Distance (ENN) between *Miombo* woodland patches, which was relatively consistent in 1990 but progressively increased in subsequent years (Figure 8E). By 2024, ATHR and LTHD showed the greatest distances between *Miombo* woodland patches and signaling increased fragmentation, while BKHD, MKHD, and THR also exhibited notable increases. These trends underscore the intensifying fragmentation of *Miombo* woodlands, emphasizing the urgent need for conservation measures to protect and restore remaining *Miombo* woodland habitats. This includes implementing sustainable land use practices, enhancing reforestation efforts, and promoting policies that mitigate the drivers of fragmentation, such as deforestation and agricultural expansion.

4. Discussion

4.1. Methodology

This study employed a multiscale analysis using Landsat imagery and various landscape metrics—such as class area, patch number, and edge density—to examine deforestation dynamics [64]. The use of multiple metrics is essential for a comprehensive understanding of deforestation given its multifaceted nature, which cannot be captured through a single metric alone [65,66]. To interpret these metrics effectively, a decision tree was incorporated, aiding in the differentiation between anthropogenic and natural land cover transformations and in linking observed changes to their underlying causes. To account for the temporal variability of spatial transformation processes, this study refined the temporal resolution to 5 to 6 years [62,67,68].

Landsat images, with a 30 m resolution, are well-suited for regional-scale analysis, providing valuable insights into land cover trends and changes over time [16,69]. The capability of Landsat to detect vegetation changes at this scale is crucial for mapping and quantifying the impacts of human activities on forest ecosystems, which is vital for effective management and conservation efforts [70]. Furthermore, the free availability of Land-sat data makes it a particularly valuable tool for monitoring landscape dynamics in regions with limited surveillance resources [71,72].

This study concentrated on key land cover classes, including agriculture, urbanization, savannas, and *Miombo* woodlands, to assess landscape transformation and its impact on deforestation. While the combination of grasslands and wooded savannas—distinct ecosystems—may present limitations, this approach was justified for capturing general deforestation trends at a regional scale. Future research could benefit from more detailed, finer-scale analyses to address these limitations. The literature supports that both grasslands and wooded savannas are often of anthropogenic origin, with their prominence in the landscape growing in response to human activities [22,73].

While the study's methodology has certain limitations, such as the broad categorization of land cover types, it has provided robust insights into deforestation dynamics by leveraging a combination of metrics, refined temporal resolution, and extensive data sources. These methodological choices have not compromised the interpretation of the results but rather enhanced the understanding of regional-scale deforestation trends and their drivers. The ground truth data collection conducted in June and July 2024 validated the reliability of reference points for the changing and stable areas identified on the 2020–

2024 map, focusing on land use classes, such as open *Miombo* woodlands, savannas, and agricultural and built-up lands. Using GPS, we compared field observations with the results of Landsat image reclassifications.

4.2. Anthropogenic Pressures and Extent of the Hierarchical Changes in the Spatio-Temporal Pattern of Deforestation in Lualaba Province

Our study highlights the significant expansion of savannas, agricultural fields, and urban areas in Lualaba Province, driven primarily by the region's abundant natural resources, such as fertile soils and mineral deposits like copper and cobalt [41]. These resources have attracted considerable investments in agriculture and mining, resulting in notable sectoral growth [20,74]. This pattern mirrors similar trends observed in southern central Angola [75], where resource wealth also fueled economic expansion.

Improved road networks have further facilitated access to rural areas, thereby promoting agricultural and mining activities and enabling rural populations to migrate to urban centers for employment and services [16,20]. This phenomenon of rural to urban migration is evident in Mekelle, Ethiopia, where a favorable investment climate has similarly driven increased urban land demand [76]. The growing national and international demand for rosewood and mining products has additionally stimulated expansion in these sectors [74,77,78].

The need to increase agricultural land to satisfy rising food demands has led to the conversion of *Miombo* woodlands into maize and cassava fields, particularly in the Katangense copper belt [20,79]. Simultaneously, large- and small-scale mining operations have contributed to deforestation through infrastructure development and extraction [16]. Unplanned urban expansion has further exacerbated this issue by converting *Miombo* woodland lands into residential, commercial, and industrial zones, resulting in significant habitat fragmentation and loss. For example, Cabala et al. [18] documented the conversion of 177.5 km^2 of *Miombo* woodland to bare soil and settlements in the Lubumbashi plain between 2005 and 2011. Economic challenges have driven populations to build makeshift housing near *Miombo* woodlands, often with inadequate infrastructure, highlighting a pattern of prioritizing immediate survival over long-term resource sustainability.

The socio-economic and environmental dynamics of Lualaba Province have been profoundly influenced by the rise and fall of industries, especially mining and agriculture, coupled with shifting governance structures. During the 1980s, the cessation of operations by Kisenge Manganese, a key employer in agricultural territories, and the discontinuation of Tabacongo's activities before 1997 significantly impacted local employment and the regional economy [41]. The collapse of Gécamines in the 1990s led many locals to shift from wage labor to subsistence activities, including *Miombo* woodland resource exploitation and small-scale agriculture [20]. This economic decline forced rural populations into makeshift housing near forests, often lacking infrastructure [71].

Lualaba's deforestation trends are reflective of broader national and regional patterns, where political instability and economic fluctuations have significant impacts on land use. For example, socio-political turmoil in the DRC from 1990 to 2001 led to a reduction in large-scale logging and a slowdown in urban expansion due to insecurity and limited infrastructure investment. The creation of Lualaba Province in 2015, however, accelerated deforestation as infrastructure development, urbanization, and economic activities surged, especially around mining sites [21,26,73]. During the period of socio-political instability, minimal agricultural growth and limited urban infrastructure investments slowed deforestation rates [71]. The political instability also decreased foreign investments in logging, resulting in a halving of deforestation rates during this time [80].

The liberalization of the mining sector in 2002 generally led to an increase in large-scale mining operations, particularly for copper and cobalt, which contributed to vegetation fragmentation in Lualaba Province [21]. Despite this, provincial policies requiring mining companies to cultivate agricultural fields have led to increased agricultural land [20,21]. This trend is also reflected in the rise of private farming enterprises with large landholdings. However, a notable decrease in deforestation was observed following the global financial crisis in 2008, as reduced mining activity led to lower demand for forest land for mining infrastructure [81]. The establishment of the new province in 2015, conversely, increased deforestation rates due to heightened infrastructure development, urbanization, and expanded economic activities [20]. In this new province, characterized by widespread poverty and low electricity access, forest resources are heavily exploited for charcoal production [82,83], which remains crucial for cooking and heating [73]. Despite this, the carbonization yield in the region remains low [84].

Our findings demonstrate that deforestation in Lualaba occurs primarily through the fragmentation of *Miombo* woodland patches, which aligns with previous studies [18,20]. Forest fragmentation results from roads, infrastructure development, agricultural expansion, and urban growth [85]. This fragmentation often leads to smaller, isolated forest patches as intact areas become increasingly scarce [86]. As anthropogenic pressure mounts, remaining forest patches are lost, as observed in the Lufira Biosphere [26]. On the other hand, savanna patches are expanding due to extensive agricultural practices, charcoal production, and bushfires [19]. The transformation of *Miombo* woodland areas into savannas is driven by agricultural activities and bushfires, contributing to the growing presence of savannas in Lualaba Province [22,87,88].

Uncontrolled urbanization often leads to acquiring new land rather than densifying existing areas due to the complexity and cost of land regularization and infrastructure investment [89]. This practice is particularly prevalent in regions with minimal urban development, such as DRC, where urban growth tends to concentrate around mining sites where construction on bare soil is more straightforward [23]. This approach not only exacerbates inefficient land use but also poses significant health risks due to exposure to environmental hazards, including trace metals from mining operations [90].

Deforestation is more severe in areas practicing shifting cultivation compared to mining regions. Shifting cultivation, or slash and burn agriculture, involves periodic cutting and burning of forest plots, leading to temporary and recurrent deforestation [91,92]. This practice exerts pressure on protected areas due to inadequate monitoring [26,72,93]. Agricultural lands are more accessible and less regulated than mining zones, which are subject to stricter environmental controls [74]. Consequently, agricultural lands are more prone to deforestation driven by local economic interests [94]. Despite their protected status, forest cover in these areas declines due to poor management, demographic pressure, and illegal activities [93]. Corruption and enforcement challenges exacerbate these issues, confirming that agriculture remains a leading cause of deforestation [95–97].

The deforestation rates in Lualaba Province are significantly higher than the national average of 0.4% per year. This elevated rate is attributed to intensified logging, agricultural and mining expansion, illegal activities, and weak forest governance. Despite national conservation efforts, local factors contribute to higher deforestation rates in provinces like Lualaba. Protected areas face intense pressure from subsistence agriculture, artisanal mining, and fuelwood collection, compounded by outdated monitoring resources [98]. This situation mirrors issues observed in Kasenga [99], Butembo [100], and Zambia [101], leading to severe deforestation in areas like the Lufira Biosphere Reserve [26]. At larger scales, commercial agriculture and mining drive deforestation, although provincial or national conservation measures can help mitigate these effects [21,102,103]. Governance of forest resources in Lualaba remains a challenge, with the ICCN (Congolese Institute for Nature Conservation) and its partners focusing mainly on parks, while other protected areas remain vulnerable [26]. The intensification of forest fragmentation has created isolated patches, threatening biodiversity.

Our study results show that the annual deforestation rate in the Basse Kando hunting reserve is concerning. First, the Basse Kando protected area is geographically situated between two major urban centers, Kolwezi and Fungurume. These economically booming cities are experiencing rapid population growth, leading to increased demand for forest products, particularly firewood and construction materials. This creates constant pressure on the surrounding forests, including those within the protected area, as they provide a relatively cheap and accessible supply. Second, the presence of mining concessions within the protected area exacerbates deforestation. Mining activities, which require cleared spaces for extraction, are accompanied by numerous informal commercial activities that cluster around mining sites. These include restaurants that largely depend on firewood for cooking meals for workers, as well as small-scale agricultural operations that support the mining population. However, in the Lubudi territory, the rising number of artisanal mining sites and the expansion of exploited areas significantly contribute to deforestation, justifying the highest annual rate of deforestation recorded. Artisanal mining practices, often unregulated and labor-intensive, necessitate forest clearing to access mineral deposits or establish temporary camps. Deforested lands are rarely restored post-extraction, leading to long-term degradation of local ecosystems.

Forest fragmentation profoundly impacts biodiversity, climate mitigation, and restoration efforts. As forest patches become smaller and more isolated, species that once thrived in continuous, expansive habitats face increased vulnerability. Fragmented forests often result in diminished habitat diversity and connectivity, which can lead to population declines and increased extinction risks for many species. This fragmentation disrupts migration corridors and breeding grounds, thereby impacting ecological interactions and ecosystem health. Additionally, the loss of large forested areas compromises the forest's ability to sequester carbon effectively, reducing its role in climate regulation and exacerbating global warming. The fragmentation also challenges restoration efforts, as reforestation projects must contend with the difficulties of restoring connectivity and ecological function across fragmented landscapes.

Vegetation fires exacerbate fragmentation by destroying large forest areas and creating bare land, reducing the ability of remaining patches to recover, and hindering biodiversity and climate mitigation efforts. Useni et al. [88] observed this in Kundelungu National Park, where fires increasingly affected savannas between 2001 (70 km^2 in the Integral Zone, 239 km^2 in the Annex Zone) and 2022 (76 km^2 and 744 km^2, respectively), limiting their potential to evolve into forests.

4.3. Implications for the Conservation of Landscape and Forest Ecosystems in Lualaba

Our study highlights the urgent need for sustainable land management in agriculture-oriented territories, which are increasingly susceptible to deforestation, including within protected areas. By employing remote sensing techniques and landscape metrics, we have gained significant insights into deforestation dynamics in Lualaba Province, revealing the critical impact of mining, urbanization, and agricultural expansion on *Miombo* woodland ecosystems.

The findings underscore the necessity for policies that promote sustainable land use and conservation. Given the evidence of significant forest fragmentation and loss driven by anthropogenic activities, it is crucial to implement measures that focus on reforestation and ecosystem restoration using indigenous species, supported by financial incentives for sustainable agricultural practices. Global initiatives aiming to restore up to 700 million hectares of forest over the next 50 years [104] align with local successes, such as the agroforestry project near Lubumbashi, which has rehabilitated 350 hectares with *Acacia auriculiformis* [105].

To prevent further agricultural encroachment, establishing buffer zones around protected areas is essential. Collaborative management between state wildlife agencies and NGOs can enhance the effectiveness of these protected zones [106]. Implementing regulated agricultural reserves can mitigate deforestation from intensive farming practices, thus addressing the limitations of current land allocation models controlled by local authorities [78].

For impoverished communities, adopting sustainable agricultural practices, such as agroforestry, crop rotation, and water conservation, is crucial. The success of *Acacia auriculiformis* plantations on the Batéké plateau, which produce significant quantities of charcoal, cassava, maize, and honey [107], exemplifies the benefits of these practices. Improved methods, such as using adapted seeds and integrated pest management, can further reduce forest pressure. Creating ecological corridors similar to the Ambositra-Vondrozo Corridor in Madagascar can enhance connectivity between forest patches and facilitate species movement [108].

Effective conservation efforts require strong local involvement. The lack of community engagement in Lubumbashi has exacerbated deforestation, whereas active participation has supported forest regeneration in Burundi [109]. Implementing awareness programs, environmental education, and capacity-building initiatives is essential. Partnerships with international organizations and NGOs can provide vital support [110–112], while media campaigns and educational programs can further increase environmental awareness [113].

Strengthening environmental legislation and enforcement is critical for protecting forest areas and curbing illegal activities. This includes improving monitoring within protected areas, implementing strict access and land use measures, and imposing penalties for illegal deforestation [114]. Addressing governance challenges, including corruption, requires transparency and accountability mechanisms [115,116]. The recovery of forest areas in the Bururi Forest Reserve, due to restrictions on human activities and increased ranger presence, illustrates the positive impact of rigorous enforcement [109].

Looking ahead, future research should focus on several key areas. First, conducting socio-economic surveys could provide a more comprehensive understanding of long-term trends and the intricate nature of human–environment interactions. Additionally, further studies are needed to evaluate the effectiveness of different reforestation and conservation strategies across various socio-economic contexts. Investigating the impacts of specific agricultural practices on forest ecosystems and exploring innovative land management techniques will be crucial. Lastly, examining the role of local governance and community engagement in forest conservation can offer insights into improving policy implementation and enhancing environmental stewardship.

Our methodological approach integrating remote sensing and landscape metrics has advanced the understanding of deforestation dynamics in Lualaba Province. Despite limitations, such as the spatial resolution of remote sensing data and the absence of socio-economic surveys, our results offer valuable insights into the complex interactions between human activities and forest ecosystems. This study emphasizes the need for immediate conservation actions and the implementation of sustainable land management practices to preserve remaining forest ecosystems. By identifying key areas for policy intervention and future research, our findings contribute meaningfully to the broader discourse on forest conservation and sustainable development. Collaborative efforts will be essential to safeguard the ecological integrity of Lualaba's forest ecosystems for future generations.

5. Conclusions

Our study utilized a methodological approach that integrated remote sensing techniques with landscape analysis methods to quantify the multiscale spatio-temporal dynamics of *Miombo* woodland ecosystems within the Lualaba Province. This approach allowed us to confirm a notable increase in deforested and fragmented areas, aligning with our general objective to investigate these dynamics. The observed changes were attributed to the expansion of anthropogenic activities, such as mining, urbanization, and agriculture, which have significantly altered the structure and connectivity of *Miombo* woodland ecosystems over time. Our findings demonstrated that deforestation, characterized by the fragmentation of *Miombo* woodland patches, is primarily influenced by the expansion of savannas and agricultural practices, alongside urban development.

Of particular concern is the vulnerability of agricultural territories to this phenomenon, including designated protected areas that were also impacted. While our study provided valuable insights, we faced limitations, including the spatial resolution of remote sensing data and the absence of socio-economic surveys, which could have offered a more comprehensive understanding of long-term trends and the complex human–environment interactions.

Despite these limitations, our results unveiled a complex pattern of deforestation, emphasizing the critical need for immediate actions to preserve the remaining *Miombo* woodland ecosystems in the Lualaba region. This includes implementing land conservation policies, adopting sustainable agricultural practices, and enforcing stricter forest regulations. Furthermore, future analyses should focus on the fragmentation and degradation of natural ecosystems, emphasizing the importance of land use dynamics and their impacts on forest fragmentation and degradation. Collaborative actions are necessary to safeguard the ecological richness and functionality of the forest ecosystems within the Lualaba province for future generations.

Author Contributions: Y.U.S.: conceptualization, methodology, and writing—original draft preparation; M.M.M.: methodology, writing—original draft preparation, and data curation; J.K.T., D.K.K. and F.M.: writing—review and editing; J.B.: supervision, writing—original draft, and funding acquisition. All authors have read and agreed to the published version of the manuscript.

Funding: This work is supported by the Academy for Research and Higher Education, Commission for Development Cooperation-CONV-21-519 (Belgium).

Data Availability Statement: The authors confirm that all data supporting the findings of this study are available within the article.

Acknowledgments: The authors would like to thank the development research project "Capacity building for the sustainable management of the *Miombo* clear forest through the assessment of the environmental impact of charcoal production and the improvement of forest resource management practices (CHARLU)" and the administrative services of the Lualaba's territories for the facilities provided.

Conflicts of Interest: The authors have no conflicts of interest to declare. All co-authors have reviewed and approved the contents of the manuscript, and there are no financial interests to report. We confirm that the submission represents original work and is not currently under review by any other publication.

References

1. Portillo-Quintero, C.; Sanchez-Azofeifa, A.; Calvo-Alvarado, J.; Quesada, M.; do Espirito Santo, M.M. The role of tropical dry forests for biodiversity, carbon and water conservation in the neotropics: Lessons learned and opportunities for its sustainable management. *Reg. Environ. Chang.* **2015**, *15*, 1039–1049. [CrossRef]
2. Hasnat, G.T.; Hossain, M.K. Global overview of tropical dry forests. In *Handbook of Research on the Conservation and Restoration of Tropical Dry Forests*; IGI Global: Hershey, PA, USA, 2020; p. 23.
3. Seiler, C. *The Sensitivity of Tropical Forests to Climate Variability and Change in Bolivia*; Wageningen University and Research: Wageningen, The Netherlands, 2014.
4. Sinha, P.G. Effect of climate change on tropical dry forests. In *Research Anthology on Environmental and Societal Impacts of Climate Change*; IGI Global: Hershey, PA, USA, 2022; pp. 1132–1149.
5. Teshome, J.Y. Role of Dry Forests in Rural Socio-economic Development in Sub-Saharan Africa. *J. Acad. Ind. Res. (JAIR)* **2019**, *8*, 29.
6. Dlamini, C.S. Contribution of forest ecosystem services toward food security and nutrition. In *Zero Hunger*; Springer International Publishing: Cham, Germany, 2020; pp. 179–196.
7. Djoudi, H.; Vergles, E.; Blackie, R.R.; Koame, C.K.; Gautier, D. Dry forests, livelihoods and poverty alleviation: Understanding current trends. *Int. For. Rev.* **2015**, *17*, 54–69. [CrossRef]
8. Miles, L.; Newton, A.C.; DeFries, R.S.; Ravilious, C.; May, I.; Blyth, S.; Gordon, J.E. A Global Overview of the Conservation Status of Tropical Dry Forests. *J. Biogeogr.* **2006**, *33*, 491–505. [CrossRef]
9. Blackie, R.; Baldauf, C.; Gautier, D.; Gumbo, D.; Kassa, H.; Parthasarathy, N.; Sunderland, T. *Tropical Dry Forests: The State of Global Knowledge and Recommendations for Future Research*; Cifor: Bogor, Indonesia, 2014; 41p. [CrossRef]
10. Frost, P. The ecology of *miombo* woodlands. In *The Miombo in Transition: Woodlands and Welfare in Africa*; Center for International Forestry Research: Bogor, Indonesia, 1996; 266p.
11. Campbell, B.M.; Angelsen, A.; Cunningham, A.; Katerere, Y.; Sitoe, A.; Wunder, S. *Miombo Woodlands—Opportunities and Barriers to Sustainable Forest Management*; Center for International Forestry Research: Bogor, Indonesia, 2007.
12. Jew, E.K.; Dougill, A.J.; Sallu, S.M.; O'Connell, J.; Benton, T.G. *Miombo* Woodland under Threat: Consequences for Tree Diversity and Carbon Storage. *For. Ecol. Manag.* **2016**, *361*, 144–153. [CrossRef]

13. Syampungani, S.; Chirwa, P.W.; Akinnifesi, F.K.; Sileshi, G.; Ajayi, O.C. The *Miombo* Woodlands at the Cross Roads: Potential Threats, Sustainable Livelihoods, Policy Gaps and Challenges. *Nat. Resour. Forum* **2009**, *33*, 150–159. [CrossRef]
14. Chidumayo, E.N. Changes in *Miombo* Woodland Structure under Different Land Tenure and Use Systems in Central Zambia. *J. Biogeogr.* **2002**, *29*, 1619–1626. [CrossRef]
15. Ribeiro, N.S.; Matos, C.N.; Moura, I.R.; Washington-Allen, R.A.; Ribeiro, A.I. Monitoring Vegetation Dynamics and Carbon Stock Density in *Miombo* Woodlands. *Carbon Balance Manag.* **2013**, *8*, 11. [CrossRef]
16. Potapov, P.V.; Turubanova, S.A.; Hansen, M.C.; Adusei, B.; Broich, M.; Altstt, A.; Mane, L.; Justice, C.O. Quantifying forest cover loss in Democratic Republic of the Congo, 2000–2010, with Landsat ETM+data. *Remote Sens. Environ.* **2012**, *122*, 106–116. [CrossRef]
17. Kabulu Djibu, J.P.; Bamba, I.; Munyemba Kankumbi, F.; Defourny, P.; Vancutsem, C.; Nyembwe, N.S.; Bogaert, J. Analyse de la structure spatiale des forêts au Katanga. *Ann. Fac. Sci. Agron. L'université Lubumbashi* **2008**, *1*, 12–18.
18. Cabala, K.S.; Useni, S.Y.; Sambieni, K.R.; Bogaert, J.; Munyemba, K.F. Dynamique des écosystèmes forestiers de l'Arc CuprifèreKatangais en République Démocratique du Congo. Causes, Transformations spatiales et ampleur. *Tropicultura* **2017**, *35*, 192–202.
19. Useni, S.Y.; Malaisse, F.; Kaleba, S.C.; Kankumbi, F.M.; Bogaert, J. Le rayon de déforestation autour de la ville de Lubumbashi (Haut-Katanga, RD Congo): Synthèse. *Tropicultura* **2017**, *35*, 215–221.
20. Khoji, M.K.; N'Tambwe, N.D.-D.; Malaisse, F.; Waselin, S.; Sambiéni, K.R.; Cabala, K.S.; Munyemba, K.F.; Bastin, J.-F.; Bogaert, J.; Useni, S.Y. Quantification and Simulation of Landscape Anthropization around the Mining Agglomerations of SoutheasternKatanga (DR Congo) between 1979 and 2090. *Land* **2022**, *11*, 850. [CrossRef]
21. Dupin, L.; Nkono, C.; Burlet, C.; Muhashi, F.; Vanbrabant, Y. Land cover fragmentation using multi-temporal remote sensing on major mine sites in Southern Katanga (Democratic Republic of Congo). *Adv. Remote Sens.* **2013**, *2*, 127–139. [CrossRef]
22. Malaisse, F. *How to Live and Survive in Zambezian Open Forest (Miombo Ecoregion)*; Les Presses Agronomiques de Gembloux: Gembloux, Belgium, 2010.
23. Chai, B.; Seto, K.C. Conceptualizing and Characterizing Micro-Urbanization: A New Perspective Applied to Africa. *Landsc. Urban Plan.* **2019**, *190*, 103595. [CrossRef]
24. Useni, Y.S.; Malaisse, F.; Yona, J.M.; Mwamba, T.M.; Bogaert, J. Diversity, use and management of household-located fruit trees in two rapidly developing towns in Southeastern DR Congo. *Urban For. Urban Green.* **2021**, *63*, 127220. [CrossRef]
25. Gnassou, L. The End of the Commodities Super-Cycle and its Implications for the Democratic Republic of Congo in Crisis. *Afr. Policy J.* **2016**, *12*, 77.
26. Useni, S.Y.; Muteya, H.K.; Bogaert, J. *Miombo* woodland, an ecosystem at risk of disappearance in the Lufira Biosphere Reserve (Upper Katanga, DR Congo)? A 39-years analysis based on Landsat images. *Glob. Ecol. Conserv.* **2020**, *24*, e01333.
27. Lele, N.; Joshi, P.K. Analyzing Deforestation Rates, Spatial Forest Cover Changes and Identifying Critical Areas of Forest Cover Changes in North-East India during 1972–1999. *Environ. Monit. Assess.* **2009**, *156*, 159–170. [CrossRef]
28. Hein, L.; Van Ierland, E. Efficient and Sustainable Management of Complex Forest Ecosystems. *Ecol. Model.* **2006**, *190*, 351–366. [CrossRef]
29. Huang, Y.; Chen, Z.X.; Tao, Y.U.; Huang, X.Z.; Gu, X.F. Agricultural remote sensing big data: Management and applications. *J. Integr. Agric.* **2018**, *17*, 1915–1931. [CrossRef]
30. Nagendra, H.; Lucas, R.; Honrado, J.P.; Jongman, R.H.; Tarantino, C.; Adamo, M.; Mairota, P. Remote sensing for conservation monitoring: Assessing protected areas, habitat extent, habitat condition, species diversity, and threats. *Ecol. Indic.* **2013**, *33*, 45–59. [CrossRef]
31. Rawat, J.S.; Kumar, M. Monitoring land use/cover change using remote sensing and GIS techniques: A case study of Hawalbagh block, district Almora, Uttarakhand, India. *Egypt. J. Remote Sens. Space Sci.* **2015**, *18*, 77–84. [CrossRef]
32. Achard, F.; DeFries, R.; Eva, H.; Hansen, M.; Mayaux, P.; Stibig, H.J. Pan-Tropical Monitoring of Deforestation. *Environ. Res. Lett.* **2007**, *2*, 045022. [CrossRef]
33. Achard, F.; Stibig, H.J.; Eva, H.D.; Lindquist, E.J.; Bouvet, A.; Arino, O.; Mayaux, P. Estimating Tropical Deforestation from Earth Observation Data. *Carbon Manag.* **2010**, *1*, 271–287. [CrossRef]
34. Tucker, C.J.; Townshend, J.R. Strategies for Monitoring Tropical Deforestation Using Satellite Data. *Int. J. Remote Sens.* **2000**, *21*, 1461–1471. [CrossRef]
35. De Sy, V.; Herold, M.; Achard, F.; Asner, G.P.; Held, A.; Kellndorfer, J.; Verbesselt, J. Synergies of multiple remote sensing data sources for REDD+monitoring. *Curr. Opin. Environ. Sustain.* **2012**, *4*, 696–706. [CrossRef]
36. Frohn, R.C. *Remote Sensing for Landscape Ecology: New Metric Indicators for Monitoring, Modeling, and Assessment of Ecosystems*; CRC Press: Boca Raton, FL, USA, 2018; pp. 1–350.
37. Imbernon, J.; Branthomme, A. Characterization of landscape patterns of deforestation in tropical rain forests. *Int. J. Remote Sens.* **2001**, *22*, 1753–1765. [CrossRef]
38. Crowley, M.A.; Cardille, J.A. Remote sensing's recent and future contributions to landscape ecology. *Curr. Landsc. Ecol. Rep.* **2020**, *5*, 45–57. [CrossRef]
39. Van Engelen, V.W.P.; Verdoodt, A.; Dijkshoorn, K.; Van Ranst, E. *Soil and Terrain Data Base of Central African*; SOTERCAF, Version 1.0; FAO: Rome, Italy, 2006; 22p.

40. INS (Institut National de la Statistique). *Anuaire Statistique RDC 2022*; Ministère National du Plan: Kinshasa, Democratic Republic of the Congo, 2022; 433p.
41. Katz-Lavigne, S. Artisanal copper mining and conflict at the intersection of property rights and corporate strategies in the Democratic Republic of Congo. *Extract. Ind. Soc.* **2019**, *6*, 399–406. [CrossRef]
42. Roy, D.P.; Wulder, M.A.; Loveland, T.R.; Woodcock, C.E.; Allen, R.G.; Anderson, M.C.; Zhu, Z. Landsat-8: Science and product vision for terrestrial global change research. *Remote Sens. Environ.* **2014**, *145*, 154–172. [CrossRef]
43. Chander, G.; Markham, B.L.; Helder, D.L. Summary of current radiometric calibration coefficients for Landsat MSS, TM, ETM+, and EO-1 ALI sensors. *Remote Sens. Environ.* **2009**, *113*, 893–903. [CrossRef]
44. Choate, M.J.; Rengarajan, R.; Storey, J.C.; Lubke, M. Geometric calibration updates to Landsat 7 ETM+ instrument for Landsat Collection 2 products. *Remote Sens.* **2021**, *13*, 1638. [CrossRef]
45. Storey, J.; Choate, M.; Lee, K. Landsat 8 operational land imager on-orbit geometric calibration and performance. *Remote Sens.* **2014**, *6*, 11127–11152. [CrossRef]
46. Vermote, E.; Justice, C.; Claverie, M.; Franch, B. Preliminary analysis of the performance of the Landsat 8/OLI land surface reflectance product. *Remote Sens. Environ.* **2016**, *185*, 46–56. [CrossRef]
47. Chen, J.; Zhu, X.; Vogelmann, J.E.; Gao, F.; Jin, S. A simple and effective method for filling gaps in Landsat ETM+SLC-off images. *Remote Sens. Environ.* **2011**, *115*, 1053–1064. [CrossRef]
48. Zoran, M.A.; Zoran, L.F.V.; Dida, A.I. Forest vegetation dynamics and its response to climate changes. In *Remote Sensing for Agriculture, Ecosystems, and Hydrology XVIII*; SPIE: Bellingham, WA, USA, 2016; Volume 9998, pp. 598–608. [CrossRef]
49. Gorelick, N.; Hancher, M.; Dixon, M.; Ilyushchenko, S.; Thau, D.; Moore, R. Google Earth Engine: Planetary-scale geospatial analysis for everyone. *Remote Sens. Environ.* **2017**, *202*, 18–27. [CrossRef]
50. Chaudhary, A.; Kolhe, S.; Kamal, R. An improved random forest classifier for multi-class classification. *Inf. Process. Agric.* **2016**, *3*, 215–222. [CrossRef]
51. Olofsson, P.; Foody, G.M.; Herold, M.; Stehman, S.V.; Woodcock, C.E.; Wulder, M.A. Good practices for estimating area and assessing accuracy of land change. *Remote Sens. Environ.* **2014**, *148*, 42–57. [CrossRef]
52. Cochran, W.G. *Sampling Techniques*; John Wiley and Sons: New York, NY, USA, 1977.
53. Schuster, C.; Schmidt, T.; Conrad, C.; Kleinschmit, B.; Forster, M. Grassland habitat mapping by intra-annual time series analysis—Comparison of RapidEye and TerraSAR-X satellite data. *Int. J. Appl. Earth Obs. Geoinf.* **2015**, *34*, 25–34. [CrossRef]
54. Strahler, A.H.; Boschetti, L.; Foody, G.M.; Friedl, M.A.; Hansen, M.C.; Herold, M.; Mayaux, P.; Morisette, J.T.; Woodcock, C.E. *Global Land Cover Validation: Recommendations for Evaluation and Accuracy Assessment of Global Land Cover Maps*; European Commission: Luxembourg, 2006.
55. Olofsson, P.; Foody, G.M.; Stehman, S.V.; Woodcock, C.E. Making better use of accuracy data in land change studies: Estimating accuracy and area and quantifying uncertainty using stratified estimation. *Remote Sens. Environ.* **2013**, *129*, 122–131. [CrossRef]
56. Zhang, J.; Qu, M.; Wang, C.; Zhao, J.; Cao, Y. Quantifying landscape pattern and ecosystem service value changes: A case study at the county level in the Chinese Loess Plateau. *Glob. Ecol. Conserv.* **2020**, *23*, e01110. [CrossRef]
57. Wang, H.; Zhang, M.; Wang, C.; Wang, K.; Wang, C.; Li, Y.; Zhou, Y. Spatial and temporal changes of landscape patterns and their effects on ecosystem services in the Huaihe River Basin, China. *Land* **2022**, *11*, 513. [CrossRef]
58. McGarigal, K. *FRAGSTATS Help*; University of Massachusetts: Amherst, MA, USA, 2015; 182p.
59. Fahrig, L. Habitat fragmentation: A long and tangled tale. *Glob. Ecol. Biogeogr.* **2019**, *28*, 33–41. [CrossRef]
60. Haddad, N.M.; Brudvig, L.A.; Clobert, J.; Davies, K.F.; Gonzalez, A.; Holt, R.D.; Townshend, J.R. Habitat fragmentation and its lasting impact on Earth's ecosystems. *Sci. Adv.* **2015**, *1*, e1500052. [CrossRef] [PubMed]
61. Hansen, M.C.; Potapov, P.V.; Moore, R.; Hancher, M.; Turubanova, S.A.; Tyukavina, A.; Townshend, J.R. High-resolution global maps of 21st-century forest cover change. *Science* **2013**, *342*, 850–853. [CrossRef]
62. Bogaert, J.; Ceulemans, R.; Salvador-Van, E.D. Decision tree algorithm for detection of spatial processes in landscape transformation. *Environ. Manag.* **2004**, *33*, 62–67. [CrossRef]
63. de Haulleville, T.; Rakotondrasoa, O.L.; Rakoto Ratsimba, H.; Bastin, J.F.; Brostaux, Y.; Verheggen, F.J.; Rajoelison, G.L.; Malaisse, F.; Poncelet, M.; Haubruge, É.; et al. Fourteen years of anthropization dynamics in the Uapaca bojeri Baill. *For. Madagascar. Landsc. Ecol. Eng.* **2018**, *14*, 135–146. [CrossRef]
64. Wang, J.; Yang, X. A hierarchical approach to forest landscape pattern characterization. *Environ. Manag.* **2012**, *49*, 64–81. [CrossRef]
65. Lausch, A.; Herzog, F. Applicability of landscape metrics for the monitoring of landscape change: Issues of scale, resolution and interpretability. *Ecol. Indic.* **2002**, *2*, 3–15. [CrossRef]
66. Bogaert, J.; Vranken, I.; André, M. Anthropogenic effects in landscapes: Historical context and spatial pattern. In *Biocultural Landscapes: Diversity, Functions and Values*; Springer: Dordrecht, The Netherlands, 2014; pp. 89–112.
67. TV, R.; Setturu, B.; Chandran, S. Geospatial analysis of forest fragmentation in Uttara Kannada District, India. *For. Ecosyst.* **2016**, *3*, 10.
68. Martinez Pardo, J.; Saura, S.; Insaurralde, A.; Di Bitetti, M.S.; Paviolo, A.; De Angelo, C. Much more than forest loss: Four decades of habitat connectivity decline for Atlantic Forest jaguars. *Landsc. Ecol.* **2023**, *38*, 41–57. [CrossRef]
69. Stellmes, M.; Udelhoven, T.; Röder, A.; Sonnenschein, R.; Hill, J. Dryland observation at local and regional scale—Comparison of Landsat TM/ETM+ and NOAA AVHRR time series. *Remote Sens. Environ.* **2010**, *114*, 2111–2125. [CrossRef]

70. Vogelmann, J.E.; Gallant, A.L.; Shi, H.; Zhu, Z. Perspectives on monitoring gradual change across the continuity of Landsat sensors using time-series data. *Remote Sens. Environ.* **2016**, *185*, 258–270. [CrossRef]
71. Gorsevski, V.; Kasischke, E.; Dempewolf, J.; Loboda, T.; Grossmann, F. Analysis of the impacts of armed conflict on the Eastern Afromontane forest region on the South Sudan—Uganda border using multitemporal Landsat imagery. *Remote Sens. Environ.* **2012**, *118*, 10–20. [CrossRef]
72. Koy, J.K.; Wardell, D.A.; Mikwa, J.F.; Kabuanga, J.M.; Monga Ngonga, A.M.; Oszwald, J.; Doumenge, C. Dynamics of deforestation in the Yangambi biosphere reserve (Democratic Republic of Congo): Spatial and temporal variability in the last 30 years. *Bois For. Trop.* **2019**, *341*, 15–28.
73. Khoji, M.H.; Nghonda, D.-d.N.; Kalenda, F.M.; Strammer, H.; Kankumbi, F.M.; Malaisse, F.; Bastin, J.-F.; Sikuzani, Y.U.; Bogaert, J. Mapping and Quantification of *Miombo* Deforestation in the Lubumbashi Charcoal Production Basin (DR Congo): Spatial Extent and Changes between 1990 and 2022. *Land* **2023**, *12*, 1852. [CrossRef]
74. Mwitwa, J.; German, L.; Muimba-Kankolongo, A.; Puntodewo, A. Governance and sustainability challenges in landscapes shaped by mining: Mining-forestry linkages and impacts in the Copper Belt of Zambia and the DR Congo. *For. Policy Econ.* **2012**, *25*, 19–30. [CrossRef]
75. Schneibel, A.; Stellmes, M.; Röder, A.; Frantz, D.; Kowalski, B.; Haß, E.; Hill, J. Assessment of spatio-temporal changes of smallholder cultivation patterns in the Angolan *Miombo* belt using segmentation of Landsat time series. *Remote Sens. Environ.* **2017**, *195*, 118–129. [CrossRef]
76. Fenta, A.A.; Yasuda, H.; Haregeweyn, N.; Belay, A.S.; Hadush, Z.; Gebremedhin, M.A.; Mekonnen, G. The dynamics of urban expansion and land use/land cover changes using remote sensing and spatial metrics: The case of Mekelle City of northern Ethiopia. *Int. J. Remote Sens.* **2017**, *38*, 4107–4129. [CrossRef]
77. Molinario, G.; Hansen, M.; Potapov, P.; Tyukavina, A.; Stehman, S. Contextualizing landscape-scale forest cover loss in the Democratic Republic of Congo (DRC) between 2000 and 2015. *Land* **2020**, *9*, 23. [CrossRef]
78. Mpanda, M.M.; Muteya, H.K.; Nghonda, D.-D.N.; Sambiéni, K.R.; Malaisse, F.; Kaleba, S.C.; Bogaert, J.; Sikuzani, Y.U. Uncontrolled Exploitation of Pterocarpus tinctorius Welw. and Associated Landscape Dynamics in the Kasenga Territory: Case of the Rural Area of Kasomeno (DR Congo). *Land* **2022**, *11*, 1541. [CrossRef]
79. Molinario, G.; Hansen, M.C.; Potapov, P.V. Forest cover dynamics of shifting cultivation in the Democratic Republic of Congo: A remote sensing-based assessment for 2000–2010. *Environ. Res. Lett.* **2015**, *10*, 094009. [CrossRef]
80. Ernst, C.; Mayaux, P.; Verhegghen, A.; Bodart, C.; Christophe, M.; Defourny, P. National forest cover change in Congo Basin: Deforestation, reforestation, degradation and regeneration for the years 1990, 2000 and 2005. *Glob. Chang. Biol.* **2013**, *19*, 1173–1187. [CrossRef]
81. Antonarakis, A.S.; Pacca, L.; Antoniades, A. The effect of financial crises on deforestation: A global and regional panel data analysis. *Sustain. Sci.* **2022**, *17*, 1037–1057. [CrossRef]
82. Trefon, T.; Hendriks, T.; Kabuyaya, N.; Ngoy, B. L'économie politique de la filière du charbon de bois à Kinshasa et à Lubumbashi. In *Appui Stratégique à la Politique de Reconstruction Post-Conflit en RDC*; IOB; GIZ; University of Antwerp: Antwerpen, Belgium, 2010.
83. Kabulu, D.J.-P.; Vranken, I.; Bastin, J.-F.; Malaisse, F.; Nyembwe, N.S.; Useni, S.Y.; Ngongo, L.M.; Bogaert, J. Approvisionnement En Charbon de Bois Des Ménages Lushois: Quantités, Alternatives et Conséquences. In *Anthropisation des Paysages Katangais*; Bogaert, J., Colinet, G., Mahy, G., Eds.; Presses Universitaires de Liège: Liège, Belgium, 2018; pp. 297–311.
84. Mukendi, N.K.; Muteya, H.K.; Nghonda, D.D.N.T.; Berti, F.; Useni Sikuzani, Y.; Ndjibu, L.N.; Bogaert, J. Quantification and Determinants of Carbonization Yield in the Rural Zone of Lubumbashi, DR Congo: Implications for Sustainable Charcoal Production. *Forests* **2024**, *15*, 554. [CrossRef]
85. Bogaert, J.; Bamba, I.; Koffi, K.J.; Sibomana, S.; Djibu, J.P.K.; Champluvier, D.; Visser, M.N. Fragmentation of forest landscapes in Central Africa: Causes, consequences and management. In *Patterns and Processes in Forest Landscapes: Multiple Use and Sustainable Management*; Lafortezza, R., Chen, J., Sanesi, G., Crow, T.R., Eds.; Springer: Dordrecht, The Netherlands, 2008; pp. 67–87. [CrossRef]
86. Fischer, R.; Taubert, F.; Müller, M.S.; Groeneveld, J.; Lehmann, S.; Wiegand, T.; Huth, A. Accelerated forest fragmentation leads to critical increase in tropical forest edge area. *Sci. Adv.* **2021**, *7*, eabg7012. [CrossRef]
87. Useni, S.Y.; Mpanda Mukenza, M.; Khoji Muteya, H.; Cirezi Cizungu, N.; Malaisse, F.; Bogaert, J. Vegetation Fires in the Lubumbashi Charcoal Production Basin (The Democratic Republic of the Congo): Drivers, Extent and Spatiotemporal Dynamics. *Land* **2023**, *12*, 2171. [CrossRef]
88. Useni Sikuzani, Y.; Khoji Muteya, H.; Langunu, S.; Gerardy, A.; Bogaert, J. Amplification of anthropogenic pressure heavily hampers natural ecosystems regeneration within the savanization halo around Lubumbashi city (Democratic Republic of Congo). *Int. J. Environ. Sci. Nat. Resour.* **2019**, *17*, 555958. [CrossRef]
89. Mama, A.; Bamba, I.; Sinsin, B.; Bogaert, J.; De Cannière, C. Déforestation, savanisation et développement agricole des paysages de savanes-forêts dans la zone soudano-guinéenne du Bénin. *Bois For. Trop.* **2014**, *322*, 66–75. [CrossRef]
90. Banza, C.L.N.; Nawrot, T.S.; Haufroid, V.; Decrée, S.; De Putter, T.; Smolders, E.; Nemery, B. High human exposure to cobalt and other metals in Katanga, a mining area of the Democratic Republic of Congo. *Environ. Res.* **2009**, *109*, 745–752. [CrossRef] [PubMed]

91. Tanzito, G.; Ibanda, P.A.; Talaguma, R.; Lusanga, N.M. Slash-and-burn agriculture, the major cropping system in the region of Faradje in Democratic Republic of Congo: Ecological and socio-economic consequences. *J. Dev. Agric. Econ.* **2020**, *12*, 25–36. [CrossRef]
92. Montfort, F.; Nourtier, M.; Grinand, C.; Maneau, S.; Mercier, C.; Roelens, J.B.; Blanc, L. Regeneration capacities of woody species biodiversity and soil properties in *Miombo* woodland after slash-and-burn agriculture in Mozambique. *For. Ecol. Manag.* **2012**, *274*, 142–154. [CrossRef]
93. Useni, S.Y.; Mpanda, M.M.; Malaisse, F.; Kaseya, P.K.; Bogaert, J. The Spatiotemporal Changing Dynamics of *Miombo* Deforestation and Illegal Human Activities for Forest Fire in Kundelungu National Park, Democratic Republic of the Congo. *Fire* **2023**, *6*, 174. [CrossRef]
94. Vermeulen, C.; Dubiez, É.; Proces, P.; Diowo, M.; Yamba, Y.; Mutambwe, S.; Doucet, J.L. Enjeux fonciers, exploitation des ressources naturelles et Forêts des Communautés Locales en périphérie de Kinshasa, RDC. *Biotechnol. Agron. Société Environ.* **2011**, *15*, 651–661.
95. Phiri, D.; Mwitwa, J.; Ng'andwe, P.; Kanja, K.; Munyaka, J.; Chileshe, F.; Kwenye, J.M. Agricultural expansion into forest reserves in Zambia: A remote sensing approach. *Geocarto Int.* **2023**, *38*, 2213203. [CrossRef]
96. Dimobe, K.; Ouédraogo, A.; Soma, S.; Goetze, D.; Porembski, S.; Thiombiano, A. Identification of driving factors of land degradation and deforestation in the Wildlife Reserve of Bontioli (Burkina Faso, West Africa). *Glob. Ecol. Conserv.* **2015**, *4*, 559–571. [CrossRef]
97. Acheampong, E.O.; Macgregor, C.J.; Sloan, S.; Sayer, J. Deforestation is driven by agricultural expansion in Ghana's forest reserves. In Proceedings of the 2019 Conference on Tropical Deforestation, Accra, Ghana, 15–17 October 2019.
98. Chitonge, H.; Mfune, O. The Urban Land Question in Africa: The Case of Urban Land Conflicts in the City of Lusaka, 100 Years after Its Founding. *Habitat Int.* **2015**, *48*, 209–218. [CrossRef]
99. Useni Sikuzani, Y.; Kipili Mwenya, I.; Khoji Muteya, H.; Malaisse, F.; Cabala Kaleba, S.; Bogaert, J. Anthropogenic Pressures and Spatio-Temporal Dynamics of Forest Ecosystems in the Rural and Border Municipality of Kasenga (DRC). *Landsc. Ecol. Eng.* **2024**, *20*, 195–212. [CrossRef]
100. Kasereka, K.K.; Mweru, J.P. Gouvernance environnementale de la ville de Butembo par les services publics urbains (Nord-Kivu, République Démocratique du Congo). *Tropicultura* **2018**, *36*, 578–592.
101. Kaswamila, A.L.; Songorwa, A.N. Participatory Land-Use Planning and Conservation in Northern Tanzania Rangelands. *Afr. J. Ecol.* **2009**, *47*, 128–134. [CrossRef]
102. Butsic, V.; Baumann, M.; Shortland, A.; Walker, S.; Kuemmerle, T. Conservation and conflict in the Democratic Republic of Congo: The impacts of warfare, mining, and protected areas on deforestation. *Biol. Conserv.* **2015**, *191*, 266–273. [CrossRef]
103. Majambu, E.; Tsayem Demaze, M.; Sufo-Kankeu, R.; Sonwa, D.J.; Ongolo, S. The effects of policy discourse on the governance of deforestation and forest degradation reduction in the Democratic Republic of Congo (DRC). *Environ. Policy Gov.* **2023**, *34*, 307–320. [CrossRef]
104. Meyer, S.E.; Callaham, M.A.; Stewart, J.E.; Warren, S.D. Invasive Species Response to Natural and Anthropogenic Disturbance. In *Invasive Species in Forests and Rangelands of the United States: A Comprehensive Science Synthesis for the United States Forest Sector*; Springer Nature: Berlin, Germany, 2021; pp. 85–110. [CrossRef]
105. Boldrini, S. Guide Technique. Plantation Agroforestière d'*Acacia auriculiformis* dans le Haut-Katanga. Master's Thesis, University of Lubumbashi, Lubumbashi, Democratic Republic of the Congo, 2017.
106. Lindsey, P.; Baghai, M.; Bigurube, G.; Cunliffe, S.; Dickman, A.; Fitzgerald, K.; Robson, A. Attracting Investment for Africa's Protected Areas by Creating Enabling Environments for Collaborative Management Partnerships. *Biol. Conserv.* **2021**, *255*, 108979. [CrossRef]
107. Bisiaux, F.; Peltier, R.; Muliele, J.C. Plantations industrielles et agroforesterie au service des populations des plateaux Batéké, Mampu, en République Démocratique du Congo. *Bois Forêts Trop.* **2009**, *301*, 21–32. [CrossRef]
108. Ramiadantsoa, T.; Ovaskainen, O.; Rybicki, J.; Hanski, I. Large-scale habitat corridors for biodiversity conservation: A forest corridor in Madagascar. *PLoS ONE* **2015**, *10*, e0132126. [CrossRef]
109. Havyarimana, F.; Masharabu, T.; Kouao, J.K.; Bamba, I.; Nduwarugira, D.; Bigendako, M.J.; De Canniere, C. La dynamique spatiale de la forêt située dans la réserve naturelle forestière de Bururi au Burundi. *Tropicultura* **2017**, *35*, 158–172.
110. Zikargae, M.H.; Woldearegay, A.G.; Skjerdal, T. Empowering rural society through non-formal environmental education: An empirical study of environment and forest development community projects in Ethiopia. *Heliyon* **2022**, *8*, e09127. [CrossRef]
111. Bare, M.; Kauffman, C.; Miller, D.C. Assessing the impact of international conservation aid on deforestation in sub-Saharan Africa. *Environ. Res. Lett.* **2015**, *10*, 125010. [CrossRef]
112. Khoji, M.H.; Mokuba, H.K.; Sambieni, K.R.; Sikuzani, Y.U.; Moyene, A.B.; Bogaert, J. Évaluation de la dynamique spatiale des forêts primaires au sein du Parc national de la Salonga sud (RD Congo) à partir des images satellites Landsat et des données relevées in situ. *VertigO-La Rev. Électronique Sci. L'environnement* **2024**, *24*. [CrossRef]
113. Mapira, J. Zimbabwe's Environmental Education Programme and Its Implications for Sustainable Development. Ph.D. Thesis, Stellenbosch University, Stellenbosch, South Africa, 2014.
114. Galabuzi, C.; Eilu, G.; Nabanoga, G.N.; Turyahabwe, N.; Mulugo, L.; Kakudidi, E.; Sibelet, N. Has the evolution process of forestry policies in Uganda promoted deforestation? *Int. For. Rev.* **2015**, *17*, 298–310. [CrossRef]

115. Khoji, M.H.; Mpanda, M.M.; Mwenya, I.K.; Malaisse, F.; Mukendi, N.K.; Bastin, J.F.; Bogaert, J.; Useni, S.Y. Protected area creation and its limited effect on deforestation: Insights from the Kiziba-Baluba Hunting Domain (DR Congo). *Trees For. People* **2024**, *18*, 100654. [CrossRef]
116. Klein, B.; Mullard, S.; Ahamadi, K.; Mara, P.; Mena, J.; Nourdine, S.; Maraina, A.V. (Re) Interpreting corruption in local environments: Disputed definitions, contested conservation, and power plays in Northern Madagascar. *Political Geogr.* **2023**, *107*, 102973. [CrossRef]